


Organic Anion Transporter 2–Mediated Hepatic Uptake Contributes to the Clearance of High-Permeability–Low-Molecular-Weight Acid and Zwitterion Drugs: Evaluation Using 25 Drugs^S

Emi Kimoto, Sumathy Mathialagan, Laurie Tylaska, Mark Niosi, Jian Lin, Anthony A. Carlo, David A. Tess, and  Manthena V. S. Varma

Medicine Design, Worldwide Research and Development, Pfizer Inc., Groton, Connecticut

Received July 12, 2018; accepted August 15, 2018

ABSTRACT

High-permeability–low-molecular-weight acids/zwitterions [i.e., extended clearance classification system class 1A (ECCS 1A) drugs] are considered to be cleared by metabolism with a minimal role of membrane transporters in their hepatic clearance. However, a marked disconnect in the in vitro–in vivo (IVIV) translation of hepatic clearance is often noted for these drugs. Metabolic rates measured using human liver microsomes and primary hepatocytes tend to underpredict. Here, we evaluated the role of organic anion transporter 2 (OAT2)–mediated hepatic uptake in the clearance of ECCS 1A drugs. For a set of 25 ECCS 1A drugs, in vitro transport activity was assessed using transporter-transfected cells and primary human hepatocytes. All but two drugs showed substrate affinity to OAT2, whereas four (bromfenac, entacapone, fluorescein, and nateglinide) also showed OATP1B1 activity in transfected cells. Most of these

drugs (21 of 25) showed active uptake by plated human hepatocytes, with rifamycin SV (pan-transporter inhibitor) reducing the uptake by about 25%–95%. Metabolic turnover was estimated for 19 drugs after a few showed no measurable substrate depletion in liver microsomal incubations. IVIV extrapolation using in vitro data was evaluated to project human hepatic clearance of OAT2-alone substrates considering 1) uptake transport only, 2) metabolism only, and 3) transporter–enzyme interplay (extended clearance model). The transporter–enzyme interplay approach achieved improved prediction accuracy (average fold error = 1.9 and bias = 0.93) compared with the other two approaches. In conclusion, this study provides functional evidence for the role of OAT2-mediated hepatic uptake in determining the pharmacokinetics of several clinically important ECCS 1A drugs.

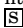
Introduction

We recently proposed a framework called extended clearance classification system (ECCS) to predict the rate-determining clearance mechanism of drugs or new molecular entities using simple molecular properties, including ionization state and molecular weight and in vitro membrane permeability (Varma et al., 2015; El-Kattan and Varma, 2018). According to this validated system, ECCS class 1A drugs (i.e., high-permeability–low-mol. wt. <400-Da acids/zwitterions) are thought to be cleared primarily by metabolism as the rate-determining step. However, despite the predominance of cytochrome 450 (P450)-and/or uridine 5′-diphospho-glucuronosyltransferase (UGT)-mediated metabolic pathways, many studies have indicated a marked disconnect in the in vitro–in vivo (IVIV) translation for

this class of drugs. That is, metabolic rates measured by substrate depletion and/or metabolite formation in the incubations of human liver microsomes and human hepatocytes considerably underpredict human hepatic clearance of ECCS 1A drugs (Obach, 1999; Brown et al., 2007; Bowman and Benet, 2016; Wood et al., 2017). Several previous studies discussed plausible causes for IVIV disconnect in hepatic clearance as measured using hepatocytes and liver microsomes, which include permeation rate limitation, diffusion through unstirred water layer, suboptimal substrate concentration, reagent handling, and assay methods (Hallifax and Houston, 2012; Poulin et al., 2012; Bowman and Benet, 2016; Wood et al., 2017). Although the causes are thought to be multifactorial, empirical correction of prediction bias has been suggested as a pragmatic approach for pharmacokinetic predictions in drug discovery (Hallifax and Houston, 2012; Poulin et al., 2012; Wood et al., 2017).

Membrane transporters play a key role in the absorption, distribution, clearance, and elimination of drugs (Shitara

<https://doi.org/10.1124/jpet.118.252049>.

 This article has supplemental material available at jpet.aspetjournals.org.

ABBREVIATIONS: AFE, average fold error; CL_{int}, intrinsic clearance; CL_{int, h}, intrinsic hepatic clearance; CL_{int, met}, intrinsic metabolic clearance; CL_{plasma, h}, plasma hepatic clearance; ECCS, extended clearance classification system; HBSS, Hanks' balanced salt solution; HLM, human liver microsomes; IVIV, in vitro–in vivo; LC-MS/MS, liquid chromatography–tandem mass spectrometry; MDCK, Madin-Darby canine kidney (cells); OAT, organic anion transporter; OATP, organic anion-transporting polypeptide; P450, cytochrome P450; PBPK, physiologically based pharmacokinetic; PS_{active}, active uptake clearance; PS_{passive}, passive clearance; REF, relative expression factor; SLC, solute carrier; UGT, uridine 5′-diphospho-glucuronosyltransferase.

et al., 2006; Giacomini et al., 2010; El-Kattan and Varma, 2018). Emphasis has been given to hepatic uptake clearance mediated by organic anion transporting polypeptides (OATPs), where many high-molecular-weight acids/zwitterions (ECCS class 1B/3B) are shown to be substrates (Giacomini et al., 2010; Shitara et al., 2013; Varma et al., 2015, 2017b). OAT2, a member of solute carrier 22A (SLC22A7), is expressed in the liver and kidney and is known to transport several xenobiotics and endogenous compounds (e.g., creatinine and cGMP) (Lepist et al., 2014; Shen et al., 2017). Although protein abundance of OAT2 in the human liver is relatively similar to that of other major uptake transporters, such as OATP1B, Na⁺-taurocholate cotransporting polypeptide, and organic cation transporter (OCT)1 (Nakamura et al., 2016; Vildhede et al., 2018), little is known about its role in the clinical pharmacokinetics of drugs (Shen et al., 2017). We recently identified the role of OAT2-mediated hepatic uptake in the clearance of tolbutamide and R- and S-warfarin, which were previously assumed to be cleared by metabolism involving P450 2C9/19 (Bi et al., 2018a,b). Mechanistic in vitro studies and physiologically based pharmacokinetic (PBPK) modeling and simulations demonstrated the significance of OAT2-CYP2C interplay in their clinical pharmacokinetics (Bi et al., 2018,b). Given that these drugs are high-permeability–low-molecular-weight acids, we hypothesized that OAT2-mediated hepatic uptake contributes to the clearance of ECCS class 1A drugs.

The main objective of this investigation was to evaluate the role of transporter-mediated hepatic uptake in the pharmacokinetics of high-permeability–low-molecular-weight acids and zwitterions. To this end, for a set of about 25 ECCS class 1A drugs (Varma et al., 2015), in vitro transport activity was characterized using transporter-transfected cells and primary human hepatocytes, and metabolic clearance was measured in human liver microsome (HLM) incubations supplemented with cofactors for oxidation and glucuronidation pathways. Moreover, IVIV extrapolation was evaluated to quantitatively predict human hepatic clearance considering the uptake and metabolic clearances separately and assuming transporter-enzyme interplay (extended clearance model).

Materials and Methods

Chemicals and Reagents. Rosuvastatin was purchased from Carbosynth (Compton, UK). R- and S-warfarin and rifamycin SV were purchased from Sigma-Aldrich (St. Louis, MO). [³H]-cGMP was purchased from PerkinElmer Life Sciences (Boston, MA). All other test compounds were obtained from the Pfizer Chemical inventory system. In VitroGro-HT and CP hepatocyte media were purchased from Bioreclamation/VT (Baltimore, MD). Collagen I-coated 24-well plates were obtained from Corning (Kennebunk, ME). Dulbecco's modified Eagle's medium (DMEM), fetal bovine serum, nonessential amino acids, GlutaMAX-1, sodium pyruvate, penicillin, and streptomycin solution were obtained from Invitrogen (Life Technologies, Carlsbad, CA). Cryopreserved human plateable hepatocytes lot Hu8246 (female Caucasian, 37 years old) were obtained from Thermo Fisher Scientific (Carlsbad, CA). BCA protein assay kit was purchased from Pierce/Biotechnology (Rockford, IL). NP-40 protein lysis buffer was purchased from Thermo-Fisher (Franklin, MA). Human embryonic kidney (HEK)293 cells expressing human OATP1B1 were obtained from Absorption Systems (Exton, PA). HEK293 cells stably transfected with human OAT2(tv-1) were obtained from the laboratory of Ryan Pelis (Dalhousie University, Halifax, Canada).

In Vitro Transport Studies Using Transporter-Transfected Cells. HEK293 cells singly transfected with OATP1B1 or OAT2 and wild-type cells were seeded at a density of 0.5–1.2 × 10⁵ cells/well on BioCoat 48- or 96-well poly-D-lysine-coated plates (Corning Inc., Corning, NY), grown in DMEM containing 10% fetal bovine serum, 1% sodium pyruvate, 1% nonessential amino acids, and 1% GlutaMAX for 48 hours at 37°C, 90% relative humidity, and 5% CO₂. In addition, OAT2-HEK cells were supplemented with 1% gentamycin and hygromycin B (50 μg/ml) and OATP1B1-HEK cells were supplemented with 1% HEPES.

Methods adopted for uptake studies are similar to those previously reported by our group (Bi et al., 2017, 2018a; Mathialagan et al., 2017). Stock solutions of all compounds were made in DMSO. Cells were rinsed three times with warm uptake buffer (Hanks' balanced salt solution (HBSS) with 20 mM HEPES, pH 7.4), followed by incubating test compounds at 1 μM (or 10 μM in some cases with analytical sensitivity issues) with a final concentration of 1% DMSO. At the end of incubation (2 minutes), the cellular uptake was terminated by washing the cells four times with ice-cold transport buffer, and then the cells were lysed with 0.2 ml of 1% NP-40 in water (radiolabeled compounds) or methanol containing internal standard (nonlabeled compounds). Transporter functionality was validated using in vitro probe substrates: 0.5 μM [³H]-cGMP (OAT2) or 0.5 μM rosuvastatin (OATP1B1) as described previously (Bi et al., 2017; Mathialagan et al., 2018). Intracellular accumulation was determined either by mixing the cell lysate with scintillation fluid followed by liquid scintillation analysis (PerkinElmer Life Sciences) for radiolabeled compounds or by liquid chromatography-tandem mass spectrometry (LC-MS/MS) analysis for nonlabeled compounds. The total cellular protein content was determined using a Pierce BCA Protein Assay kit according to the manufacturer's specifications. The uptake ratio was calculated as a ratio of accumulation in the transfected cells to the accumulation in wild-type cells.

Determination of Uptake Clearance Using Short-Term Cultured Plated Human Hepatocytes. The hepatic uptake assay was performed using short-term cultured, cryopreserved human hepatocytes as described previously (Bi et al., 2017, 2018a). Briefly, plateable cryopreserved human hepatocytes (Hu8246 lot; Thermo Fisher Scientific) were thawed in a water bath at 37°C and placed on ice. The cells were then poured into In VitroGro-HT medium at 37°C at a ratio of one vial/50 ml in a conical tube. The cells were centrifuged at 50g for 3 minutes and resuspended at 0.75 × 10⁶ cells/ml in In VitroGro-CP medium. Cell viability was determined by trypan-blue exclusion and exceeded 85%. Hepatocyte suspensions were plated in collagen-coated 24-well plates at a density of 0.375 × 10⁶ cells/well in a volume of 0.5 ml/well and incubated overnight (~18 hours). Cells were first rinsed twice with HBSS or ice-cold HBSS and preincubated with HBSS in the presence or absence of 1 mM rifamycin SV or ice-cold HBSS for 10 minutes at 37°C or 4°C. After aspirating the preincubation buffer, 0.5 ml of HBSS or ice-cold HBSS containing a substrate (1 or 10 μM) was added in the presence or absence of 1 mM rifamycin SV, a pan-SLC inhibitor (Bi et al., 2017, 2018a; Mathialagan et al., 2018). The uptake was terminated at designated times (0.25, 0.5, and 1 or 0.5, 1, and 2 minutes) by adding 0.5 ml of ice-cold standard HBSS after removal of the incubation buffer. Cells were then washed three times with 0.5 ml of ice-cold HBSS. Hepatocytes were lysed with methanol containing the internal standard for LC-MS/MS quantification.

A two-compartment mathematical model (compartments representing the media and cell) was developed to estimate the intrinsic passive clearance ($PS_{passive}$) and total intrinsic active uptake clearance (PS_{active}) by simultaneously fitting the cell accumulation (A_{cell}) data in plated human hepatocytes with and without rifamycin SV (1 mM), a pan-inhibitor of active uptake transporters. This model is analogous to the method described previously to analyze transport data in other cell systems (Poirier et al., 2008). Equations 1–6 are used in this modeling process:

$$V_{ew} \frac{dC_{ew}}{dt} = -(PS_{passive} + PS_{active}) \cdot C_{ew} \cdot f_{u,ew} + PS_{passive} \cdot C_{iw} \cdot f_{u,iw} \quad (1)$$

$$V_{iw} \frac{dC_{iw}}{dt} = (PS_{passive} + PS_{active}) \cdot C_{ew} \cdot f_{u,ew} - PS_{passive} \cdot C_{iw} \cdot f_{u,iw} \quad (2)$$

$$V_{iw} = PR \cdot CpPR \cdot VpC \quad (3)$$

$$A_{cell} = (A_{iw} + A_{ew} \cdot (1 - f_{u,ew})) \cdot 1/PR \quad (4)$$

$$C_{ew} = \frac{A_{ew}}{V_{ew}} \quad (5)$$

$$C_{iw} = \frac{A_{iw}}{V_{iw}} \quad (6)$$

where, C_{ew} , C_{iw} , A_{ew} , A_{iw} , V_{ew} (0.5 ml), V_{iw} , $f_{u,iw}$, and $f_{u,ew}$ represent the concentration (C), amount (A), volume (V), and unbound fraction (f_u) of the extracellular (ew) and intracellular (iw) compartments. PR is the measured protein concentration per well, $CpPR$ is the number of cells per measured protein (1.5 million cells/mg) (Sohlenius-Sternbeck, 2006), and VpC is cell volume (2.6 μ l/million cells, internal data) measured assuming a spherical structure (17.2 μ m diameter, internal data).

In Vitro Metabolism in Human Liver Microsomes Incubations. Pooled HLMs (HLM-103 lot prepared from a mixed gender pool of 50 donors; Sekisui XenoTech, LLC, Kansas City, KS; final protein concentration, 1 mg/ml) were diluted in 0.1 M potassium phosphate buffer (pH 7.4) containing 5 mM magnesium chloride. The microsomes were then activated by adding alamethicin at a final concentration at 10 μ g/ml and allowed to remain on ice for 15 minutes (Walsky et al., 2012). The stock solutions were first prepared in DMSO (10 mM), and then subsequent substock 100 \times solutions (0.1 mM) were prepared in 50% acetonitrile:water. The final concentration of acetonitrile in the incubation was 0.5% (v/v). The total incubation volume in the experiment was 0.5 ml. The microsome and buffer mixture was then prewarmed at 37°C for 5 minutes on a heat block before the addition of both cofactors NADPH (1.3 mM) and UDPGA (5 mM). The reaction was initiated immediately, after the addition of cofactors, with compound solutions at a final concentration of 1 μ M (Kilford et al., 2009). The incubations were terminated by removing (50- μ l) aliquots of the reaction mixture at 0-, 5-, 10-, 15-, 30-, 45-, 60-, 90-, 120-, and 180-minute time points ($n = 2$ at each time point) and were added to acetonitrile (200 μ l) containing a cocktail of internal standards. The samples were then vortexed for 1 minute and centrifuged (Allegra X-12R; Beckman Coulter, Fullerton, CA) at 3000 rpm for 5 minutes. The supernatant (150 μ l) was transferred to a 96-deep-well injection block containing (150 μ l) of high-performance liquid chromatography water containing 0.2% formic acid and mixed before LC-MS/MS analysis for the disappearance of compound. The apparent metabolic intrinsic clearance ($CL_{int,met,app}$) was determined based on the substrate-depletion half-life estimated from the ratio of the peak area response of each compound to that of the internal standard, as described earlier (Di et al., 2012).

In Vitro Substrate-Depletion Assay Using Human Hepatocytes. The high-throughput human hepatocyte substrate-depletion assay was performed in a 384-well formatted as described previously (Di et al., 2012). Briefly, the cryopreserved human hepatocytes (DCM lot, 10 donor pool; Bioreclamation IVT, Westbury, NY) were thawed and resuspended in Williams' E medium supplemented with HEPES and Na_2CO_3 . The cells were counted using the trypan blue exclusion method. Test compounds were added to suspension human hepatocytes in Williams' E medium buffer and incubated at 37°C in a humidified CO_2 incubator (75% relative humidity, 5% CO_2 /air) for 4 hours. The final incubation contained 0.5 million cells/ml and 1 μ M test compound in 15- μ l total volume with 0.1% DMSO. At various time points (0, 3, 10, 30, 60, 120, and 240 minutes), an aliquot of the sample was taken and quenched with cold acetonitrile containing internal standard (CP-628374). The samples were centrifuged (Eppendorf, Hauppauge, NY) at 3000 rpm for 10 minutes at 4°C, and the

supernatants were transferred to new plates, which were sealed before performing LC-MS/MS analysis. The apparent metabolic intrinsic clearance ($CL_{int,met,app}$) was determined based on the substrate-depletion half-life estimated from the ratio of the peak area response of each compound to that of the internal standard, as described earlier (Di et al., 2012).

LC-MS/MS Analysis. Sample analysis was conducted using LC-MS/MS system comprising an AB Sciex 5500 or 6500 triple-quadrupole mass spectrometer equipped with an electrospray source (AB Sciex, Framingham, MA), Agilent Technologies Infinity 1290 liquid chromatography-tandem mass spectrometry (Santa Clara, CA), and CTC Leap autosampler (Pflugerville, TX) programmed to inject 10 μ l of sample onto an ACE 1.7- μ m Excel C18-PFP 2.1 \times 30 mm (Advanced Chromatography Technologies Ltd, Aberdeen, Scotland), Halo C18 2.7 μ m, 100 Å 2.1 \times 30 mm (Mac Mod, Chadds Ford, PA), or a Kinetex C18 2.6 μ m, 100 Å, 3 \times 30 mm (Phenomenex, Torrance, CA) analytical column. A binary gradient was used consisting of 0.1% (v/v) formic acid in water (mobile phase A) and 0.1% (v/v) formic acid in acetonitrile (mobile phase B) and monitored using the multiple reaction monitoring mode for the m/z transitions, as described in Supplemental Table 1.

Data Analysis. In vivo hepatic intrinsic clearance ($CL_{int,h}$) was calculated from human intravenous clearance data assuming the well stirred liver model in eq. 7 (Pang and Rowland, 1977):

$$CL_{int,h} = \frac{CL_{blood,h}}{f_{u,b} \cdot \left(1 - \frac{CL_{blood,h}}{Q_h}\right)} \quad (7)$$

where $CL_{blood,h} [= (CL_{plasma} - CL_{renal})/Rb]$ is the hepatic blood clearance obtained from intravenous total plasma clearance corrected for renal clearance and blood-to-plasma ratio (Rb), $f_{u,b}$ is the fraction unbound in blood [= the fraction unbound in plasma ($f_{u,p}$)/ Rb], and Q_h is hepatic blood flow (20.7 ml/min per kilogram) (Kato et al., 2003).

Predicted $CL_{int,h}$ values were calculated under three different scenarios: 1) considering total hepatic uptake alone (eq. 8) measured using plated human hepatocytes, 2) considering metabolic clearance alone (eq. 9) measured by substrate depletion in HLMs, and 3) extended clearance model (eq. 10) accounting for transporter-enzyme interplay using both uptake transport (from plated human hepatocytes) and metabolic (i.e., HLM) data (Sirianni and Pang, 1997; Liu and Pang, 2005; Shitara and Sugiyama, 2006; Camenisch and Umehara, 2012; Varma et al., 2014; Patilea-Vrana and Unadkat, 2016; Kimoto et al., 2017). A schematic of the stepwise approach used in IVIV extrapolation is given in Supplemental Fig. 1:

$$CL_{int,h} = (PS_{active} \cdot REF + PS_{passive}) \quad (8)$$

$$CL_{int,h} = CL_{int,met} \quad (9)$$

$$CL_{int,h} = (PS_{active} \cdot REF + PS_{passive}) \cdot \frac{(CL_{int,met})}{(PS_{passive} + CL_{int,met})} \quad (10)$$

PS_{active} and $PS_{passive}$ are sinusoidal intrinsic active uptake clearance and intrinsic passive uptake clearance, respectively. $CL_{int,met}$ represents the intrinsic metabolic clearance measured using HLMs coincubated with both NADPH and UDPGA. $CL_{int,met}$ is equal to the measured apparent intrinsic clearance ($CL_{int,met,app}$) divided by microsomal binding ($f_{u,mic}$) or hepatocyte binding ($f_{u,hep}$). Active basolateral and canalicular efflux was assumed to be negligible (Sirianni and Pang, 1997; Shitara et al., 2013; Varma et al., 2014). The in vitro intrinsic values were scaled assuming the following: 1.5×10^6 hepatocytes/mg of measured protein, 118×10^6 hepatocytes/g of liver, 39.8 mg microsomal protein/g of liver, 24.5 g liver/kg of body weight (Varma et al., 2013). Relative expression factor (REF)—correction for the expression difference in the hepatocytes and human liver—of 1.8 and 2.0—were applied for OAT2 and OATP1B1 substrates, respectively, based on our previous published quantitative proteomics data (Kimoto et al., 2012; Vildhede et al., 2018). The

hepatocyte lot (Hu8246) used for uptake studies showed expression levels of OAT2 similar to the median expression levels of 30 single-donor cryopreserved hepatocyte lots (Vildhede et al., 2018).

Hepatic blood and plasma clearances are calculated assuming the well-stirred liver model (eq. 11), where $CL_{\text{blood, h}} = CL_{\text{plasma, h}}/R_b$:

$$CL_{\text{blood, h}} = \frac{Q_h \cdot f_{u, b} \cdot CL_{\text{int, h}}}{Q_h + f_{u, b} \cdot CL_{\text{int, h}}} \quad (11)$$

Predictive precision and accuracy were assessed with average fold error (AFE) eq. 12 and bias eq. 13:

$$AFE = 10^{\frac{1}{N} \sum \left| \log_{10} \frac{\text{Predicted}}{\text{Observed}} \right|} \quad (12)$$

$$\text{Bias} = 10^{\frac{1}{N} \sum \log_{10} \frac{\text{Predicted}}{\text{Observed}}} \quad (13)$$

N is the number of observations.

Results

Compound Selection. In a previously published data set of 368 compounds spanning across six classes of ECCS—classified based on their ionization, molecular weight, and transcellular permeability—about 10% ($n = 36$) of compounds are binned in class 1A (Varma et al., 2015; El-Kattan et al., 2016). Human intravenous clearance and renal clearance data are available for all these drugs. Of these 36 high-permeability ($>5 \times 10^{-6}$ cm/s) and low-mol. wt. (<400 Da) acids/zwitterions, three compounds (milrinone, pralidoxime, and cinafloxacin) show predominantly renal clearance, whereas others involve hepatic clearance mechanisms. All the compounds were considered for the current study, with a few exceptions: control substances (hexobarbital and thiopental) and lack of compound availability (acenocoumarol, perindopril, and

sinitroiril). A data set of 25 compounds with in vitro hepatic uptake measurements is available after a few compounds were dropped (acetylsalicylic acid, amniosalicylic acid, dichloroacetic acid, diflunisal, milrinone, and valproic acid) owing to analytical challenges and/or low cellular accumulation in uptake studies. Of the 25, six compounds returned no measurable metabolic turnover in the HLM incubations under the experimental conditions used. Therefore, the final set of 19 compounds was considered for IVIV extrapolation of transporter-enzyme interplay via extended clearance model (Supplemental Fig. 1).

In Vitro Transport in OAT2- and OATP1B1-Transfected Cells. ECCS 1A compounds were evaluated for their substrate affinity to OAT2 and OATP1B1 using transfected HEK293 cells. All the compounds studied showed uptake ratio (i.e., ratio of accumulation in transfected cells to wild-type cells) of more than 1.5 in OAT2-HEK cells, suggesting they are actively transported by OAT2, except cinafloxacin and nateglinide (Fig. 1). Whereas 85% of compounds showed an uptake ratio of >2 , and compounds such as ibuprofen, meloxicam, R-warfarin, and sulfamethoxazole yielded uptake ratios of more than 5.

In contrast, only 4 of 25 compounds (bromfenac, entacapone, fluorescein, and nateglinide) showed an uptake ratio >1.5 in OATP1B1-HEK cells, implying that most of the compounds are not transported by OATP1B1; these four compounds are OAT2/OATP1B1 dual substrates, except nateglinide (OATP1B1 alone). Positive controls of OAT2 (cGMP) and OATP1B1 (rosuvastatin) showed robust signal, supporting the performance of the cell lines used. Diclofenac, tolbutamide, and R/S-warfarin were previously reported to be OAT2 substrates using transfected cells (Zhang et al., 2016; Bi et al., 2018a,b). On the other hand, fluorescein and

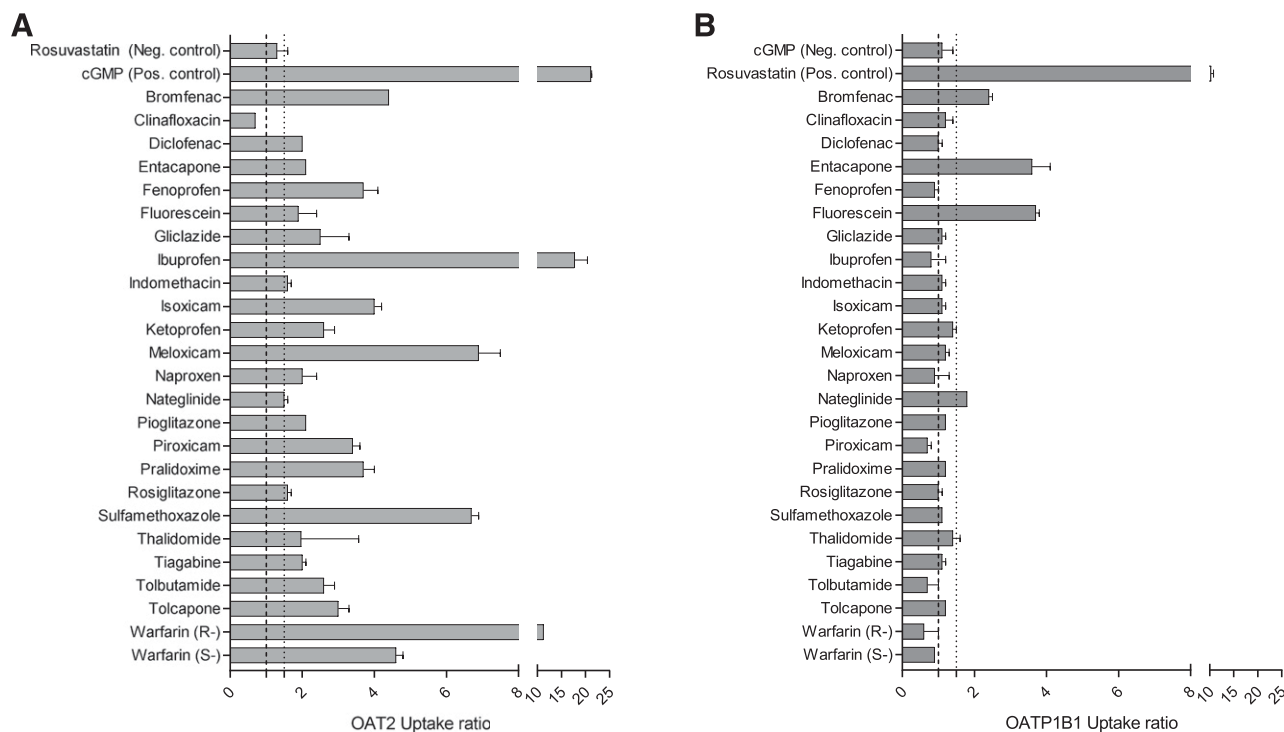


Fig. 1. OAT2- and OATP1B1-mediated transport of ECCS 1A drugs in overexpressing cells. Uptake was measured in HEK293 cells transfected with OAT2 (A) and OATP1B1 (B) and presented as the ratio to uptake in wild-type HEK293 cells. Bars and error bars represent mean and S.D. ($n = 3$). Dashed and dotted vertical lines represent the uptake ratio of 1 and 1.5, respectively. Uptake ratio >1.5 was used as the criteria for transport activity.

nateglinide were previously shown to be OATP1B1 substrates (De Bruyn et al., 2011; Takanohashi et al., 2012; Izumi et al., 2016). For all the other compounds, the noted transporter substrate affinity was previously unknown to our best knowledge.

In Vitro Uptake in Human Hepatocytes. Figure 2 shows the time-dependent uptake of ECCS class 1A drugs by human hepatocytes plated in short-term culture. Rifamycin SV (1 mM), a pan-SLC inhibitor (including OAT2 and OATP1B1) (Bi et al., 2017, 2018a; Mathialagan et al., 2018), significantly reduced the uptake of all compounds, with a few

exceptions. Clinafloxacin, naproxen, thalidomide, and tiagabine uptake was not altered by rifamycin SV under the experimental conditions used. In the case of diclofenac, pioglitazone, rosiglitazone, and tolcapone, the presence of rifamycin SV led to increased hepatocyte accumulation (data not shown). Although little is known about the stimulation of OAT2 activity, several previous studies have suggested plausible allosteric interaction for the substrate-dependent stimulation of the in vitro OATP activity in the presence of an inhibitor (Roth et al., 2011). Nonetheless, for these four drugs, hepatic uptake was significantly reduced when they

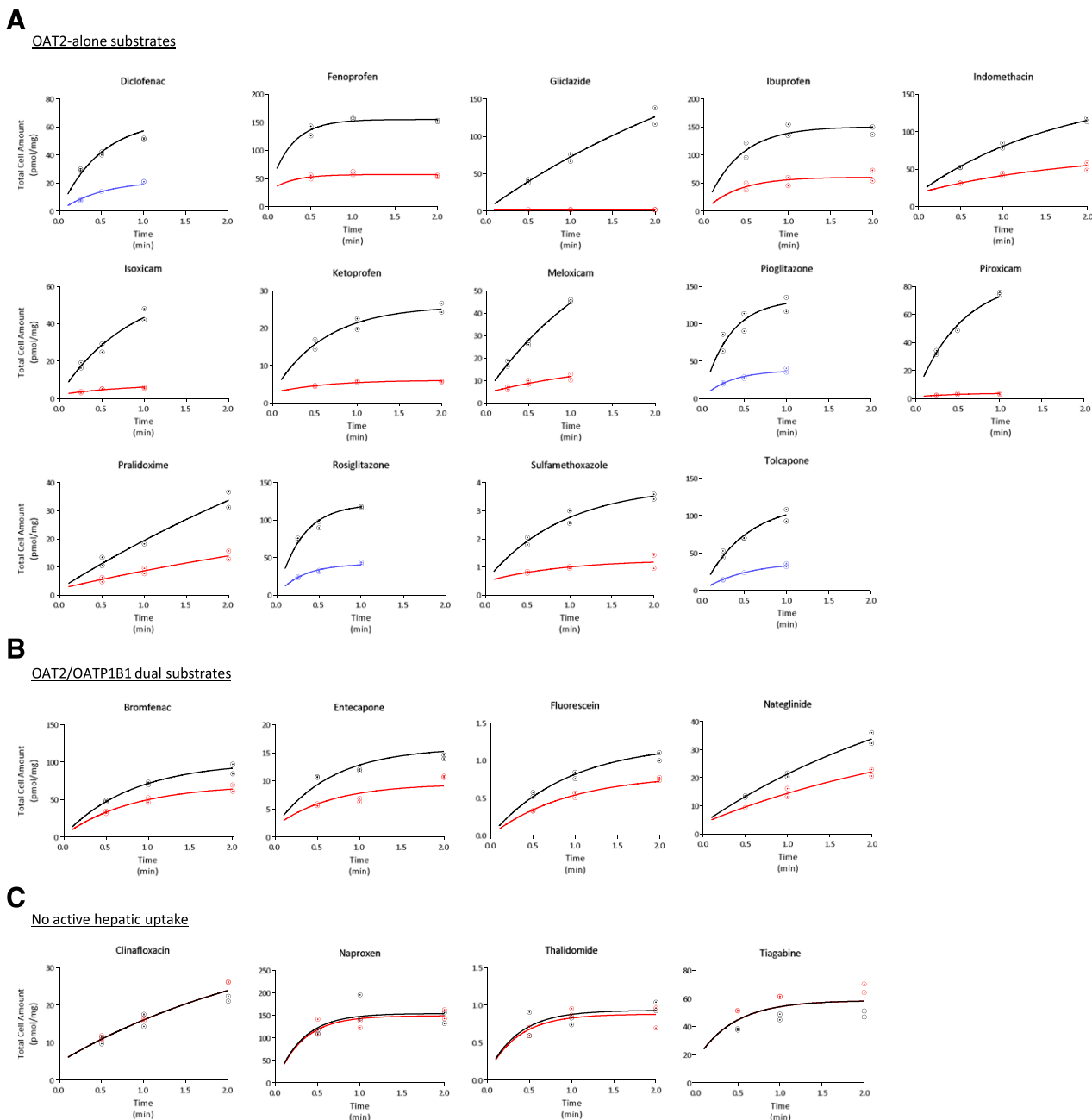


Fig. 2. Time course of cellular uptake of ECCS 1A drugs in plated human hepatocytes. Drugs were binned in three categories: OAT2-alone substrates (A), OAT2/OATP1B1 dual substrates (B), and no active hepatic uptake (C). Data points and curves represent uptake in control conditions (black) in the presence of 1 mM rifamycin SV (red) and at 4°C (blue). Curves are data-fit to the two-compartment mathematical model. Uptake rates of tolbutamide and R/S warfarin were obtained from our previous studies (Bi et al., 2018a,b). Incubation concentration is 10 μ M for fenoprofen, ibuprofen, pralidoxime, naproxen, and thalidomide and 1 μ M for all others.

were incubated on ice (4°C). Uptake time-course data were fitted to a two-compartment mathematical model to estimate the intrinsic active uptake clearance (PS_{active}) and intrinsic passive clearance (PS_{passive}), assuming 1 mM rifamycin SV (or 4°C) completely inhibited active uptake (Table 1). Estimated PS_{active} ranged from 0 (clinafloxacin) to 300 $\mu\text{l}/\text{min}$ per milligram (pioglitazone), whereas PS_{passive} ranged from 0.2 (thalidomide) to 138 $\mu\text{l}/\text{min}$ per milligram (rosiglitazone). Finally, compounds in the data set were categorized in three bins based on their transport characteristics observed with transfected cells and plated human hepatocytes: 1) OAT2 substrates with significant active uptake in human hepatocytes (referred to as OAT2-alone substrates, $n = 17$); 2) OAT2/OATP1B1 substrates with significant active hepatic uptake (OAT2/OATP1B1 dual substrates, $n = 4$); and 3) compounds with no measurable active transport in transfected and/or plated hepatocytes (i.e., no active hepatic uptake, $n = 4$). Nateglinide was recognized by only OATP1B1; however, it was included in the dual-substrates category for further data analysis. Generally, PS_{active} is higher than PS_{passive} for the OAT2-alone substrates in this set (Fig. 3A). Uptake clearance was lower for OAT2/OATP1B1 dual substrates compared with substrates for OAT2 alone.

In Vitro Metabolic Clearance in HLMs and Primary Human Hepatocytes. Intrinsic clearance of all compounds was measured by substrate-depletion method using pooled HLMs with both NADPH and UDPGA cofactors in the incubations (Table 1). The measured intrinsic clearance ($CL_{\text{int, met, app}}$) (not corrected for the microsomal binding ($f_{\text{u, mic}}$)) spanned a broad range from 1.9 (meloxicam, tolbutamide) to 140 $\mu\text{l}/\text{min}$ per milligram of protein (diclofenac). A few compounds (gliclazide, isoxicam, piroxicam, sulfamethoxazole, and R/S-warfarin) did not show measurable substrate depletion during the 180-minute incubations. In our previous study, apparent metabolic clearance in hepatocytes corrected for cell-to-media concentration (K_{puu}) was available for R/S-warfarin (Bi et al., 2018a). Microsomal binding was determined by equilibrium dialysis, and the values ranged from no binding to approximately 50% bound. It is noteworthy that the PS_{passive} measured in plated hepatocytes is equal or greater than microsomal metabolic clearance for 10 of 13 (~76%) OAT2-alone substrates (Fig. 3B).

Additionally, we measured apparent intrinsic clearance after substrate depletion in suspension human hepatocyte incubations. Values ranged from 1.6 (gliclazide) to 66.5 $\mu\text{l}/\text{min}$ per million cells (diclofenac) (Table 1). For OAT2-alone substrates, where the substrate depletion was measurable in both systems ($n = 15$), hepatocellular $CL_{\text{int, met}}$ values were on average 2.6-fold greater than the microsomal $CL_{\text{int, met}}$ (Supplemental Fig. 2).

IVIV Extrapolation to Human Hepatic Clearance. A summary of human hepatic clearance predictions from the in vitro data are presented in Table 2; and the predicted hepatic clearance values ($CL_{\text{int, h}}$ and $CL_{\text{plasma, h}}$) are plotted versus the observed clearance values in Fig. 4. IVIV extrapolation was evaluated assuming well stirred considerations under three variations: 1) uptake-determined clearance, where total hepatic uptake ($PS_{\text{active, REF}} + PS_{\text{passive}}$) was assumed to be the rate-determining step (eq. 8); 2) metabolism-determined clearance, where liver microsomal clearance was scaled alone (eq. 9); and 3) transporter-enzyme interplay, where hepatic transport and microsomal

metabolic clearance were integrated using extended clearance model (eq. 10) (Supplemental Fig. 1).

For OAT2-alone substrates, AFE for $CL_{\text{int, h}}$ predictions based on uptake-determined clearance is ~8.2, where most of the compounds are overpredicted (bias ~6.4) (Table 3). Metabolism-determined clearance alone underpredicted (AFE ~5.2 and bias ~0.20) in vivo $CL_{\text{int, h}}$ for all compounds, with a few exceptions (pioglitazone, and pralidoxime). Only 5 of 13 (38%) predictions are within 3-fold of observed values; however, prediction accuracy and bias markedly improved when using extended clearance model (AFE~1.9 and bias ~0.90). About 8 (62%) and 11 (85%) of the 13 predictions of OAT2-alone substrates are within 2-fold and 3-fold error of the observed values, respectively. Similar predictive performance could be seen for the plasma hepatic clearance predictions (Table 3).

OAT2/OATP1B1 dual substrates were considerably underpredicted in all scenarios. A scaling factor of 10.6 for active hepatic uptake (instead of OATP1B1 REF of 2.0) in the extended clearance model (eq. 10), which was previously reported by our group (Varma et al., 2014; Kimoto et al., 2017), improved clearance predictions for dual substrates to some extent (Supplemental Fig. 3). Because of limited microsomal stability data, no conclusions could be drawn for compounds with no active uptake in plated human hepatocytes.

Finally, direct scaling of intrinsic clearance measured by substrate depletion in suspension human hepatocytes reasonably predicted hepatic clearance (Fig. 5; Table 3). AFE and bias are ~2.3 and 0.63, respectively, for the OAT2-alone substrates, with ~47% and 73% predictions within 2-fold and 3-fold error, respectively. For OAT2/OATP1B1 dual substrates, this method underpredicted in vivo $CL_{\text{int, h}}$ on an average of about ~10-fold.

Discussion

This study, using a diverse set of 25 drugs, provided evidence for the functional role of OAT2-mediated hepatic uptake in the pharmacokinetics of high-permeability–low-molecular-weight acid and zwitterion drugs (i.e., ECCS 1A drugs). These drugs generally undergo extensive hepatic metabolism by CYP2C, UGTs, and other enzymes and are eliminated from the body primarily as metabolites (Varma et al., 2015; El-Kattan et al., 2016). Here, most ECCS 1A drugs demonstrated substrate affinity to OAT2 and active hepatic uptake. Clearly, hepatic clearance of OAT2-alone substrates was well predicted when using an extended clearance model, assuming transporter-enzyme interplay; however, scaling HLM clearance alone, assuming metabolism-determined clearance, showed the tendency of systemic underprediction (~5-fold). To our knowledge, this is the first study to suggest an OAT2 role in the hepatic uptake clearance and thus the pharmacokinetics for most high-permeability–low-molecular-weight acid and zwitterion drugs. These findings are of clinical importance as many such drugs are widely prescribed in a variety of therapeutic areas, including inflammation, diabetes, Parkinson disease, and thrombosis.

Based on the in vitro mechanistic studies and PBPK analyses, we have demonstrated that OAT2 plays a key role in the overall hepatic clearance of tolbutamide and R/S-warfarin, which are ECCS class 1A drugs (Bi et al., 2018a,b).

TABLE 1
Summary of drug properties and in vitro transport and metabolism measurements of the 25 high-permeability–low-molecular-weight acid and zwitterion drugs evaluated

Drug	Therapeutic Class	Permeability (10 ⁻⁶ cm/s) ^a	Mol Wt	Acidic pKa	Ionization	Uptake Transporters	Major Elimination Pathway	Main Enzyme ^e	Plasma Free Fraction (f _{u,sp}) ^d	Blood-to-Plasma Ratio ^d	Microsomal free fraction (f _{u,mic}) ^d	Hepatocyte free fraction (f _{u,HHEP}) ^d	PS _{passive} (μl/min per mg)	PHH PS _{active} (μl/min per mg)	PHH PS _{active} (μl/min per mg)	HLM CL _{met,int,app} (μl/min per mg)	HHEP CL _{met,int,app} (μl/min per M-cells)
OATP1B1/OAT2 substrates																	
Bromfenac	NSAID	17.8	334	4.1	A	OATP1B1, OAT2	Met	CYP2C9/UGT	0.002	0.55	0.29	0.40	82.7	38.1	120.8	9.3	25.1
Entacapone	Antiparkinson	6.14	305	4.0	A	OATP1B1, OAT2	Met	UGT	0.020	1.00	0.52	0.63	11.5	9.8	21.3	124.3	24.5
Fluorescein	—	5.82	332	4.5	A	OATP1B1, OAT2	Met	—	0.110	0.55	0.43	0.55	0.9	0.5	1.3	11.0	n.d.
Nateglinide	Antidiabetic	4.24	317	3.8	A	OATP1B1	Met	CYP2C9	0.011	0.55	0.86	0.91	12.6	8.1	20.7	15.3	10.8
OAT2-alone substrates																	
Diclofenac	NSAID	18.5	296	4.4	A	OAT2	Met	CYP2C9, UGT2B7	0.004	0.66	0.85	0.90	44.6	90.7	135.3	140.0	66.5
Fenoprofen	NSAID	34.2	242	4.4	A	OAT2	Met	UGT2B7	0.005	0.55	0.95	0.97	11.9	38.2	50.1	22.8	23.4
Glucoside	Antidiabetic	16.7	323	6.0	A	OAT2	Met	CYP2C9	0.050	0.55	0.90	0.94	0.1	81.1	81.2	n.d.	1.6
Ibuprofen	NSAID	29.3	206	4.4	A	OAT2	Met	CYP2C9	0.012	0.55	0.95	0.97	15.4	23.0	38.4	26.0	23.8
Indomethacin	NSAID	22.12	356	4.4	A	OAT2	Met	CYP2C9	0.012	0.66	0.77	0.84	31.2	52.4	83.6	8.4	8.3
Isoxicam	NSAID	26.9	335	3.9	A	OAT2	Met	—	0.035	0.55	0.81	0.87	6.8	63.9	70.7	n.d.	1.7
Ketoprofen	NSAID	18	254	4.1	A	OAT2	Met	CYP2C9, UGT2B7	0.021	0.55	0.86	0.91	5.6	32.6	38.2	23.9	6.5
Meloxicam	NSAID	23.9	351	3.8	A	OAT2	Met	CYP2C9/3A4	0.008	0.57	0.92	0.95	10.1	45.6	55.7	1.9	1.9
Proglitazone	Antidiabetic	23.3	356	6.1	A	OAT2	Met	CYP2C8	0.012	1.00	0.58	0.69	112.0	300.0	412.0	28.1	17.2
Piroxicam	NSAID	32.9	331	2.2	A	OAT2	Met	CYP2C9, UGT2B7	0.024	1.00	0.80	0.86	5.2	152.0	157.2	n.d.	1.7
Prairoxime	Antidote	31.9	137	7.9	A	OAT2	Renal	—	0.515	1.00	0.96	0.97	0.7	1.2	1.9	11.3	n.d.
Rosiglitazone	Antidiabetic	27.3	357	6.3	Z	OAT2	Met	CYP2C8	0.003	0.57	0.42	0.54	138.0	278.0	416.0	28.3	21.7
R-Warfarin	Anticoagulant	24.2	308	5.0	A	OAT2	Met	CYP2C9	0.013	0.59	1.00	1.00	1.1	31.1	32.2	0.2 ^h	0.7
Sulfamethoxazole	Antibacterial	8.38	253	5.6	A	OAT2	Met	CYP2C9	0.325	1.03	0.95	0.97	0.9	2.9	3.8	n.d.	n.d.
S-Warfarin	Anticoagulant	24.2	308	5.0	A	OAT2	Met	CYP2C9	0.013	0.59	1.00	1.00	0.9	22.4	23.2	0.5 ^h	1.7
Tolbutamide	Antidiabetic	31.3	270	5.1	A	OAT2	Met	CYP2C9	0.027	0.60	0.95	0.97	1.0	9.9	10.9	1.9	2.0
Tolcapone	Antiparkinson	20.9	273	5.0	A	OAT2	Met	UGT	0.002	0.55	0.59	0.70	73.5	158.0	231.5	47.2	31.7
No active hepatic uptake																	
Clinfloxacin	Antibiotic	6.84	366	5.9	Z	—	Renal	—	0.960	0.55	0.73	0.81	20.0	0.0	20.0	n.d.	n.d.
Naproxen	NSAID	22.1	230	4.3	A	OAT2	Met	UGT2B7	0.026	0.90	1.00	1.00	47.2	1.6	48.8	4.4	8.5
Thalidomide	Immunomodulatory	11.1	258	7.8	A	OAT2	Met	—	0.400	0.90	0.99	0.99	0.2	0.0	0.2	3.4	7.5
Tiagabine	Anticonvulsant	19.9	376	3.3	Z	OAT2	Met	CYP3A4	0.160	0.55	0.74	0.82	146.0	0.0	146.0	n.d.	5.2

A, Acid; HLM, human liver microsome; Met, metabolism; n.d., no measurable substrate depletion under the experimental conditions; NSAID, nonsteroidal anti-inflammatory drugs; PHH, plated human hepatocyte; Z, zwitterion.

^aMeasured in vitro across Madin Darby canine kidney (MDCK)-low efflux cells (Di et al., 2011).

^bObtained from Varma et al. (2015).

^cObtained from El-Kattan et al. (2016) and other literature.

^dMeasured by equilibrium dialysis method as described by Di et al. (2012).

^eExtracted from published literature. When data were not available, blood-to-plasma ratio of 0.55 was used.

^fMeasured by equilibrium dialysis method as described by Di et al. (2012).

^gCalculated from f_{u,mic} using the following equation (Kalvass and Maurer, 2002): f_{u,HHEP} = 1/(1 + (1/f_{u,mic} - 1) * 0.5/0.8). Where, f_{u,HHEP} was assumed equivalent to f_{u,mic} under similar assay conditions (i.e., microsomes at 1 mg/ml similar to hepatocytes at 1 million cells/ml) (Austin et al., 2005). Values, 0.5 million cells/ml represent the cell density of the hepatocytes substrate-depletion assay, and 0.8 mg/ml represent protein concentration of the f_{u,mic} assay.

^hTaken from Bi et al. (2018a).

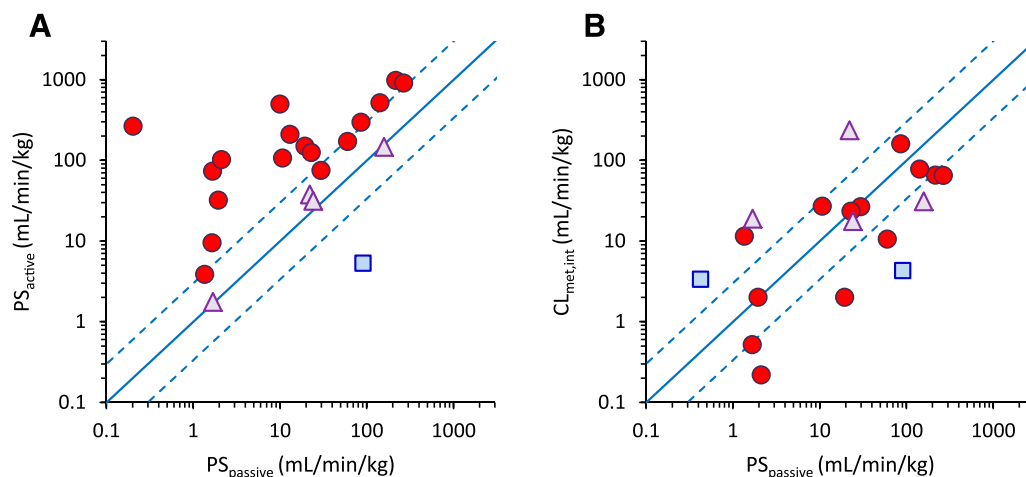


Fig. 3. Comparison of passive hepatic uptake with the active uptake clearance measured using plated human hepatocytes (A). Comparison of passive hepatic uptake measured using plated human hepatocytes with the intrinsic metabolic clearance measured in microsomal incubations (B). Circles represent OAT2-alone substrates, triangles represent OAT2/OATP1B1 dual substrates, and squares represent drugs with no measurable active uptake in human hepatocytes. Solid and dashed diagonal blue lines indicate unity and 3-fold range, respectively.

We therefore set out to investigate the role of OAT2 in the hepatic clearance for an unbiased set of 25 drugs in this class. Except for clinafloxacin and nateglinide, all drugs showed OAT2-mediated transport in transfected cells. These drugs also showed significant active uptake in primary human hepatocytes plated in short-term cultures, with a few exceptions under the experimental conditions used (clinafloxacin, naproxen, thalidomide, and tiagabine). Collectively, these *in vitro* studies provided functional evidence for active hepatic uptake driven by OAT2 for most high-permeability–low-molecular-weight acids/zwitterions. Further work is needed to understand the role of OAT2 in the clearance of other classes of drugs.

We used pooled liver microsomes to estimate *in vitro* metabolic intrinsic clearance by following substrate-depletion time course. Previous studies have shown that $CL_{int,met}$ obtained from substrate-depletion and metabolite-formation approaches are often comparable (Jones and Houston, 2004; Di et al., 2013). The presence of both cofactors, NADPH and UDPGA, in the incubations of alamethicin-activated microsomes allowed simultaneous assessment of oxidation and glucuronidation pathways (Fisher et al., 2000; Kilford et al., 2009). Moreover, values obtained here were generally consistent with the reported CL_{int} values measured using liver microsomes and hepatocytes (Obach, 1999; Brown et al., 2007); however, the microsomal $CL_{int,met}$ underpredicted *in vivo* $CL_{int,h}$ by an average of ~5-fold (bias ~0.20). This observation is also consistent with several previous reports highlighting that the *in vitro* $CL_{int,met}$ systematically underpredict the clearance of acid drugs that undergo extensive metabolism (Obach et al., 1997; Obach, 1999; Brown et al., 2007; Wood et al., 2017). No trend was noted between the predictive accuracy and the known primary enzyme involved (CYP2C vs. UGT). The current study suggests lack of consideration to OAT2-mediated hepatic uptake as a major source for IVIV disconnect noted previously in this physicochemical space.

Our recent mass spectrometry–based targeted proteomics studies indicated about 1.8-fold higher abundance of OAT2 in human liver tissue samples ($n = 52$) compared with the expression in single-donor cryopreserved hepatocytes ($n = 30$) (Vildhede et al., 2018). Similarly, in our previous studies,

~2-fold higher OATP1B1 expression was observed in liver tissues relative to the levels in cryopreserved hepatocytes (Kimoto et al., 2012). Therefore, REFs of 1.8 and 2.0 were applied when scaling *in vitro* active uptake to predict hepatic clearance for OAT2-alone substrates and OAT2/OATP1B1 substrates, respectively. We examined the sensitivity of OAT2 REF (1.8 vs. 1.0 – later assuming no correction for transporter abundance) and noted only a marginal effect on the overall predictive performance of extended clearance model (AFE 1.9 vs. 2.0; bias 0.9 vs. 0.6). However, consistent with many earlier reports (Jones et al., 2012; Ménochet et al., 2012; Varma et al., 2012b, 2014; Li et al., 2014), a scaling factor much larger than the OATP1B1 expression differences was needed to recover hepatic clearance of OATP1B1 substrates. To this end, a previously derived empirical scaling factor for the active uptake clearance ($SF_{active} \sim 10.6$) (Varma et al., 2014) provided closer predictions for the four OAT2/OATP1B1 substrates in the current data set (Supplemental Fig. 3). Collectively, direct IVIV extrapolation of OAT2-alone substrates suggests that OAT2 functional activity, unlike OATP1B1, is well preserved in cryopreserved human hepatocytes.

Depletion of parent was also assessed in pooled human hepatocytes, and the predictive performance of this system is better than that from liver microsomes (Fig. 5; Table 3). Interestingly, hepatocytes on average yielded ~2.6-fold greater substrate depletion than that measured in microsomal incubations (Supplemental Fig. 3). This is likely due to greater free cell-to-media concentrations (K_{puu}) driven by OAT2-mediated uptake in the hepatocytes. In our previous studies, we observed a K_{puu} of ~4 to 5 for R/S-warfarin in the suspension human hepatocytes (Bi et al., 2018a). Although further studies are needed to understand the reasons leading to differences in the measurements between the two systems, this study suggests that substrate-depletion in suspension human hepatocytes can be used as a pragmatic screening tool to predict hepatic clearance in this physicochemical space.

“Rapid equilibrium” between blood and liver compartments is often presumed for high-permeability drugs, resulting in the hypothesis that metabolism is the rate-determining process

TABLE 2
In vitro-in vivo extrapolation of transport and metabolism data assuming hepatic clearance is determined by total uptake, metabolism-alone, and extended clearance model
 Clearance predictions from pooled hepatocytes substrate-depletion studies were also summarized.

Drug	Intrinsic Hepatic Clearance (ml/min per kg)					Plasma Hepatic Clearance (ml/min per kg)				
	Observed ^a		Predicted			Observed ^a		Predicted		
	Hepatocyte Total Uptake	Liver Microsomes Metabolism	Extended Clearance Model	Hepatocyte Substrate Depletion	Hepatocyte Total Uptake	Liver Microsomes Metabolism	Extended Clearance Model	Hepatocyte Substrate Depletion		
Bromfenac	861.6	306.3	49.9	183.5	1.30	0.50	0.08	0.30		
Entacapone	1324.6	59.8	54.6	112.3	11.50	1.11	1.01	1.98		
Fluorescein	13.3	3.5	3.2	—	1.30	0.37	0.34	—		
Nateglinide	173.8	55.6	23.2	34.3	1.70	0.61	0.26	0.38		
Diclofenac	1220.2	391.9	255.2	213.5	3.47	1.34	0.91	0.77		
Fenoprofen	60.1	151.8	76.7	69.8	0.29	0.70	0.37	0.34		
Gliclazide	4.1	273.7	—	5.0	0.20	6.22	—	—		
Ibuprofen	71.7	107.3	50.8	71.2	0.81	1.17	0.59	0.81		
Indomethacin	102.2	236.9	35.4	28.4	1.10	2.31	0.40	0.32		
Isoxicam	2.0	228.6	—	5.7	0.07	4.70	—	0.20		
Ketoprofen	59.2	120.7	86.4	20.7	1.12	2.07	1.56	0.42		
Meloxicam	13.5	173.3	16.2	5.9	0.11	1.27	0.13	0.05		
Pioglitazone	127.3	1227.7	219.8	72.0	1.42	8.61	2.34	0.83		
Piroxicam	1.5	522.7	—	5.9	0.04	7.80	—	0.14		
Pralidoxime	8.6	5.3	4.8	—	3.65	2.42	2.20	—		
Rosiglitazone	203.9	1203.6	236.6	116.0	0.60	2.83	0.69	0.35		
R-Warfarin	3.9	107.1	8.6	1.9	0.05	1.25	0.11	0.02		
Sulfamethoxazole	1.0	11.4	—	—	0.31	3.16	—	—		
S-Warfarin	9.3	77.1	16.0	5.0	0.12	0.93	0.20	0.06		
Tolbutamide	7.9	35.2	17.5	6.1	0.21	0.88	0.45	0.16		
Tolcapone	1010.4	674.6	239.3	131.5	1.49	1.04	0.39	0.22		
Clinafloxacin	1.8	38.5	—	—	1.50	8.71	—	—		
Naproxen	3.9	94.1	4.2	24.6	0.10	2.16	0.11	0.62		
Thalidomide	6.2	0.5	0.4	21.9	2.19	0.18	0.16	5.95		
Tiagabine	11.4	281.4	—	18.2	1.57	9.09	—	2.32		

^aObserved plasma hepatic clearance was obtained from Davis et al. (2000), Delprat et al. (2002), Scordo et al. (2002), Obach et al. (2008), Varma et al. (2009), El-Kattan et al. (2016). Observed intrinsic hepatic clearance was calculated from plasma hepatic clearance using eq. 7.

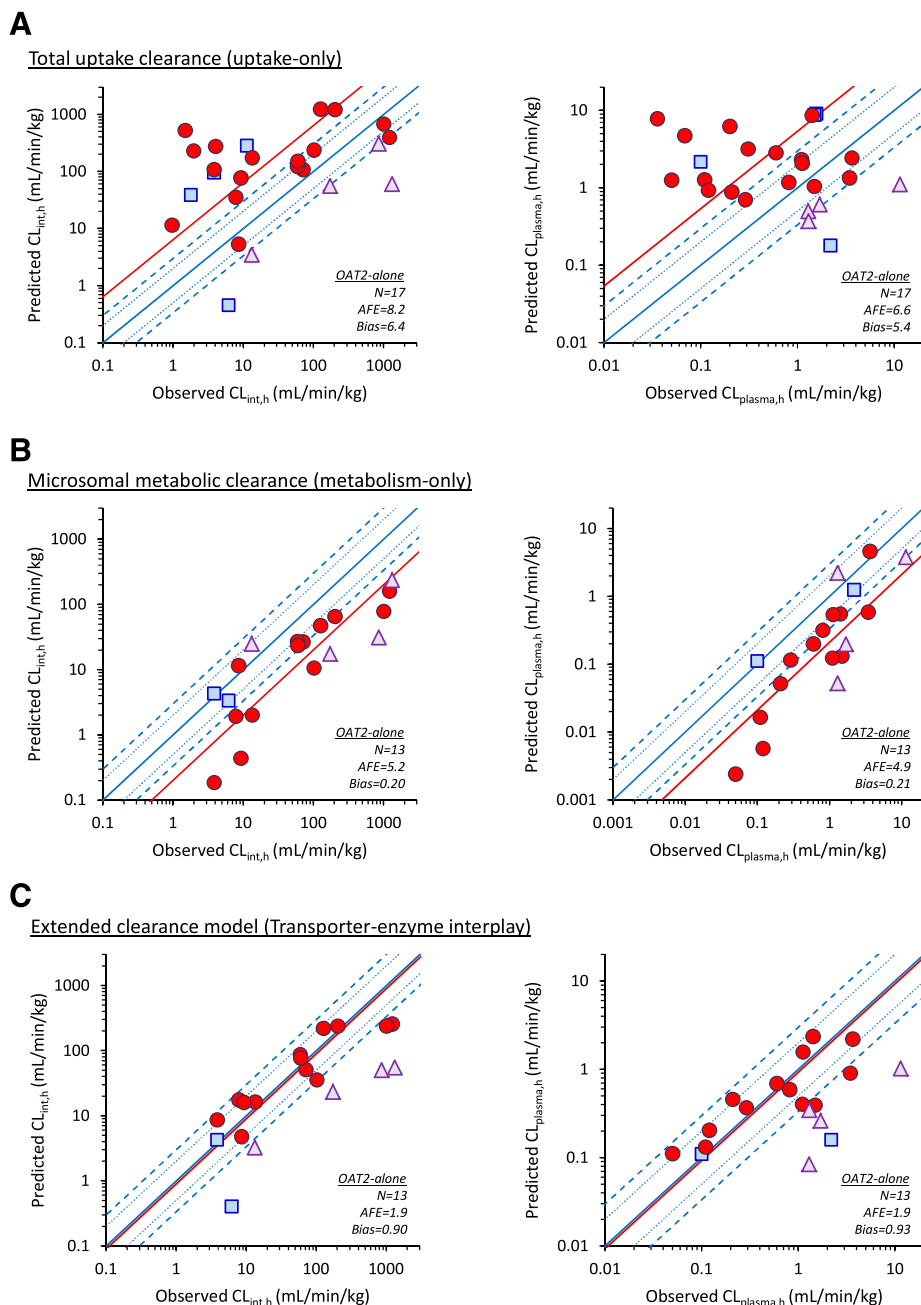


Fig. 4. IVIV extrapolation to predict human hepatic clearance of ECCS 1A drugs. Observed versus predicted hepatic clearance assuming (A) total uptake clearance alone measured using plated human hepatocytes, (B) metabolic clearance alone measured using HLMs, and (C) extended clearance model considering active and passive uptake transport and microsomal metabolic clearance. Left and right panels represent hepatic intrinsic clearance and hepatic plasma clearance, respectively. Circles represent OAT2-alone substrates, triangles represent OAT2/OATP1B1 dual substrates, and squares represent drugs with no measurable active uptake in human hepatocytes. Solid, dotted, and dashed diagonal blue lines indicate unity, 2-fold, and 3-fold range, respectively. AFE and bias (red diagonal lines) of OAT2-alone substrates are shown.

in their hepatic clearance. Transcellular permeability of the OAT2-alone substrates in our data set, measured across monolayers of Madin-Darby canine kidney (MDCK) low-efflux cells, ranged from about 8 (sulfamethoxazole) to 35×10^{-6} cm/s (fenoprofen). In the same experimental conditions, permeability of ECCS class 1B drugs (high-permeability-high-molecular-weight acids/zwitterions) span a similar range, ~ 5.5 (atorvastatin, pitavastatin) to 16×10^{-6} cm/s (repaglinide) (Varma et al., 2015; El-Kattan et al., 2016). ECCS class 1B drugs are well proven to involve OATP-mediated hepatic uptake in their systemic clearance (Shitara et al., 2013; Varma et al., 2017a). Indeed, much evidence has been presented for “uptake-determined” clearance for highly permeable and metabolically labile drugs such as atorvastatin, bosentan, and glyburide (Zheng et al., 2009; Watanabe et al.,

2010; Maeda et al., 2011; Yoshikado et al., 2017). Under similar principles, the current study demonstrated that OAT2-mediated active uptake contributes to the systemic clearance of high-permeability-low-molecular-weight acids/zwitterions. No correlation was apparent between the transcellular permeability across MDCK cell monolayers and passive uptake clearance measured in human hepatocytes (in the presence of rifamycin SV or 4°C) for the compounds in the current dataset (Supplemental Fig. 4). Drugs in our data set have a median acid pKa of ~ 4.4 (range, 2.2–7.9), implying that they exist in $>99.9\%$ ionized form (at physiologic pH 7.4), a form that is expected to have negligible passive diffusion across the cell membrane (Avdeef, 2001). This is consistent with the low passive uptake clearance and implies dependence on the active transport mechanism to achieve high total hepatic uptake noted in the

TABLE 3

Summary of predictive performance of various in vitro-in vivo extrapolation approaches employed

Bias was calculated for only OAT2-alone drugs (eq. 13).

Parameters	Intrinsic Hepatic Clearance				Plasma Hepatic Clearance			
	Hepatocyte Total Uptake	Liver Microsomes Metabolism	Extended Clearance Model	Hepatocyte Substrate Depletion	Hepatocyte Total Uptake	Liver Microsomes Metabolism	Extended Clearance Model	Hepatocyte Substrate Depletion
OAT2-alone								
n	17	13	13	15	17	13	13	15
AFE	8.2	5.2	1.9	2.3	6.6	4.9	1.9	2.2
Bias	6.4	0.20	0.90	0.63	5.4	0.21	0.93	0.65
Within 2-fold error (%) ^a	18	8	62	47	24	8	62	47
Within 3-fold error (%) ^a	35	38	85	73	41	38	85	73
OAT2/OATP1B1 dual substrates								
n	4	4	4	3	4	4	4	3
AFE	5.2	7.4	10.7	6.5	4.1	5.8	8.1	4.8
No active hepatic uptake								
n	4	2	2	3	4	2	2	3
AFE	20.5	1.4	4.1	3.3	9.7	1.4	3.9	2.9
All								
n	25	19	19	21	25	19	19	21
AFE	8.8	4.9	3.0	2.8	6.5	4.4	2.7	2.6

n, number of compounds; AFE, average fold error (eq. 12).

^aNumber of predictions within 2- and 3-fold of the observed values.

hepatocytes. Whereas cell membrane composition difference across the systems may contribute to the observed poor correlation (Simons and Ikonen, 1997), the role of uptake transporters cannot be ruled out in the transcellular permeability model (Dobson and Kell, 2008; Ahlin et al., 2009; Kell et al., 2011). Overall, potential role of uptake transporters in hepatic clearance should be duly evaluated for the acids and zwitterions irrespective of the membrane permeability across cell culture models (e.g., MDCK or Caco-2).

We observed a minimal overlap in the substrate specificity for OAT2 versus OATP1B1, which is in general agreement that OATPs preferentially accept high-MW (>400 Da) acids/zwitterions (class 1B) as substrates (Varma et al., 2012a). Of the four OATP1B1 substrates identified in the ECCS 1A space, nateglinide and fluorescein were previously reported to be OATPs substrates (De Bruyn et al., 2011; Takanoashi et al., 2012; Izumi et al., 2016), whereas this is the first report suggesting that bromfenac, a nonsteroidal

anti-inflammatory drugs for ocular inflammation, and entacapone, a catechol-O-methyltransferase inhibitor used in Parkinson disease, involve OATP1B1-mediated hepatic uptake clearance. Clinical drug-drug interaction studies with OATP inhibitors rifampicin and cyclosporine may be helpful to further define uptake-determined clearance in these cases. The MW of these four OATP1B1 substrates ranges from 305 to 334 Da. While the occurrences are low, this study suggests that low-MW acids/zwitterions may involve OATP1B1-mediated clearance.

Although a plethora of drug-drug interaction and pharmacogenetic studies have shown the relevance of CYP2C and UGT mechanisms, our findings will open the field to consider OAT2-mediated hepatic uptake as a source of variability in the pharmacokinetics and pharmacodynamics of drugs in the ECCS 1A class. According to extended clearance concept (Shitara et al., 2013; Patilea-Vrana and Unadkat, 2016; Li et al., 2014; Varma et al., 2015), the extended clearance model

Hepatocyte substrate-depletion clearance

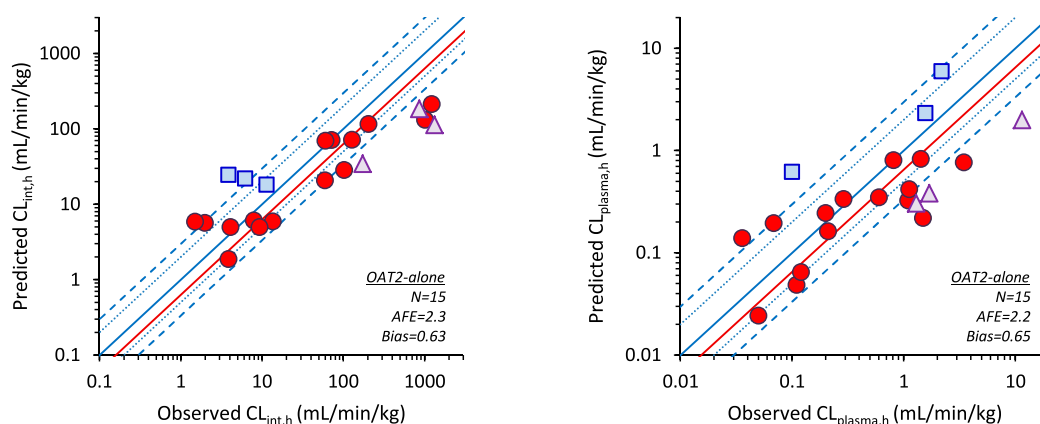


Fig. 5. Comparison of hepatic clearance predicted from intrinsic clearance measured using substrate depletion in human hepatocytes with the observed in vivo hepatic clearance. Left and right plots represent hepatic intrinsic clearance and hepatic plasma clearance, respectively. Circles represent OAT2-alone substrates, triangles represent OAT2/OATP1B1 dual substrates, and squares represent drugs with no measurable active uptake in human hepatocytes. Solid, dotted, and dashed diagonal blue lines indicate unity, 2-fold, and 3-fold range, respectively. AFE and bias (red diagonal lines) of OAT2-alone substrates are shown.

(eq. 10) is reduced such that the hepatic clearance can be approximated by $PS_{\text{uptake}} \times CL_{\text{met}}/PS_{\text{passive}}$, when $PS_{\text{passive}} > CL_{\text{int, met}}$, which is often the case for the compounds in the current data set (Fig. 3B). Therefore, functional variability in OAT2 and enzymatic metabolism can lead to variability in pharmacokinetics for these drugs. For instance, genetic polymorphism in CYP2C8 and CYP2C9 was associated with systemic clearance of many ECCS 1A drugs, including ibuprofen, piroxicam, tolbutamide, and S-warfarin (Rettie et al., 1994; Kirchheiner et al., 2002; García-Martín et al., 2004; Perini et al., 2005). For the last two drugs, we previously demonstrated that a PBPK model with permeability-limited hepatic disposition (transporter-enzyme interplay) quantitatively describes the pharmacogenetic effects when considering genotype, phenotype, and fraction metabolism by CYP2C9 (Bi et al., 2018a,b). Our preliminary literature search, however, revealed limited knowledge about the clinically relevant OAT2 inhibitors and functional polymorphic variants of *SLC22A7* (gene-encoding OAT2) (Bi et al., 2018a). Further studies are needed in these areas to assess the role of OAT2 in clinical settings. This assessment is important because changes in uptake or metabolic clearance will have a proportional impact on hepatic clearance, and a simultaneous change in both mechanisms in same direction can result in a marked change in clinical pharmacokinetics. Moreover, OAT2-mediated uptake can lead to high free liver-to-plasma concentrations (K_{puu}), which may contribute to the liver-specific pharmacologic and/or toxicologic activities. It will be of interest to understand the association between liver K_{puu} and drug-induced hepatotoxicity noted for several of the OAT2-alone substrates in our data set (e.g., diclofenac, ibuprofen, pioglitazone, piroxicam, rosiglitazone, tolcapone, etc.) (Boelsterli, 2003; Morgan et al., 2010; Chen et al., 2011).

In conclusion, our systemic evaluation provided robust evidence for the role of a previously unrecognized OAT2-mediated hepatic uptake in the clearance of several high-permeability–low-molecular-weight acid and zwitterion drugs. For this class of drugs or new chemical entities (ECCS class 1A), uptake transport characterization and considerations to transporter-enzyme interplay are important for predicting clinical pharmacokinetics and assessing variability owing to drug-drug interactions and other intrinsic and extrinsic factors.

Authorship Contributions

Participated in research design: Kimoto, Mathialagan, Tylaska, Niosi, Lin, Tess, Varma.

Conducted experiments: Kimoto, Mathialagan, Tylaska, Niosi, Lin, Carlo.

Performed data analysis: Kimoto, Mathialagan, Tylaska, Niosi, Lin, Tess, Varma.

Wrote or contributed to the writing of the manuscript: Kimoto, Mathialagan, Tylaska, Niosi, Lin, Carlo, Tess, Varma.

References

Ahlin G, Hilgendorf C, Karlsson J, Szegedy CA-K, Uhlén M, and Artursson P (2009) Endogenous gene and protein expression of drug-transporting proteins in cell lines routinely used in drug discovery programs. *Drug Metab Dispos* **37**:2275–2283.

Austin RP, Barton P, Mohamed S, and Riley RJ (2005) The binding of drugs to hepatocytes and its relationship to physicochemical properties. *Drug Metab Dispos* **33**:419–425.

Avdeef A (2001) Physicochemical profiling (solubility, permeability and charge state). *Curr Top Med Chem* **1**:277–351.

Bi YA, Lin J, Mathialagan S, Tylaska L, Callegari E, Rodrigues AD, and Varma MVS (2018a) Role of hepatic organic anion transporter 2 in the pharmacokinetics of R- and S-warfarin: in vitro studies and mechanistic evaluation. *Mol Pharm* **15**:1284–1295.

Bi YA, Mathialagan S, Tylaska L, Fu M, Keefer J, Vildhede A, Costales C, Rodrigues AD, and Varma MVS (2018b) Organic anion transporter 2 mediates hepatic uptake of tolbutamide, a CYP2C9 probe drug. *J Pharmacol Exp Ther* **364**:390–398.

Bi YA, Sciallis RJ, Lazzaro S, Mathialagan S, Kimoto E, Keefer J, Zhang H, Vildhede AM, Costales C, Rodrigues AD, et al. (2017) Reliable rate measurements for active and passive hepatic uptake using plated human hepatocytes. *AAPS J* **19**:787–796.

Boelsterli UA (2003) Diclofenac-induced liver injury: a paradigm of idiosyncratic drug toxicity. *Toxicol Appl Pharmacol* **192**:307–322.

Bowman CM and Benet LZ (2016) Hepatic clearance predictions from in vitro-in vivo extrapolation and the biopharmaceutics drug disposition classification system. *Drug Metab Dispos* **44**:1731–1735.

Brown HS, Griffin M, and Houston JB (2007) Evaluation of cryopreserved human hepatocytes as an alternative in vitro system to microsomes for the prediction of metabolic clearance. *Drug Metab Dispos* **35**:293–301.

Camenisch G and Umehara K (2012) Predicting human hepatic clearance from in vitro drug metabolism and transport data: a scientific and pharmaceutical perspective for assessing drug-drug interactions. *Biopharm Drug Dispos* **33**:179–194.

Chen M, Vijay V, Shi Q, Liu Z, Fang H, and Tong W (2011) FDA-approved drug labeling for the study of drug-induced liver injury. *Drug Discov Today* **16**:697–703.

Davis TM, Daly F, Walsh JP, Ilett KF, Beilby JP, Dusci LJ, and Barrett PHR (2000) Pharmacokinetics and pharmacodynamics of gliclazide in Caucasians and Australian Aborigines with type 2 diabetes. *Br J Clin Pharmacol* **49**:223–230.

De Bruyn T, Fattah S, Stieger B, Augustijns P, and Annaert P (2011) Sodium fluorescein is a probe substrate for hepatic drug transport mediated by OATP1B1 and OATP1B3. *J Pharm Sci* **100**:5018–5030.

Delrat P, Paraire M, and Jochemsen R (2002) Complete bioavailability and lack of food-effect on pharmacokinetics of gliclazide 30 mg modified release in healthy volunteers. *Biopharm Drug Dispos* **23**:151–157.

Di L, Feng B, Goosen TC, Lai Y, Steyn SJ, Varma MV, and Obach RS (2013) A perspective on the prediction of drug pharmacokinetics and disposition in drug research and development. *Drug Metab Dispos* **41**:1975–1993.

Di L, Keefer C, Scott DO, Strelevitz TJ, Chang G, Bi Y-A, Lai Y, Duckworth J, Fenner K, Troutman MD, et al. (2012) Mechanistic insights from comparing intrinsic clearance values between human liver microsomes and hepatocytes to guide drug design. *Eur J Med Chem* **57**:441–448.

Di L, Whitney-Pickett C, Umland JP, Zhang H, Zhang X, Gebhard DF, Lai Y, Federico JJ, III, Davidson RE, Smith R, et al. (2011) Development of a new permeability assay using low-efflux MDCKII cells. *J Pharm Sci* **100**:4974–4985.

Dobson PD and Kell DB (2008) Carrier-mediated cellular uptake of pharmaceutical drugs: an exception or the rule? *Nat Rev Drug Discov* **7**:205–220.

El-Kattan AF, Varma MV, Steyn SJ, Scott DO, Maurer TS, and Bergman A (2016) Projecting ADME behavior and drug-drug interactions in early discovery and development: application of the extended clearance classification system. *Pharm Res* **33**:3021–3030.

El-Kattan AF and Varma MVS (2018) Navigating transporter Sciences in pharmacokinetics characterization using the extended clearance classification system. *Drug Metab Dispos* **46**:729–739.

Fisher MB, Campanale K, Ackermann BL, VandenBranden M, and Wrighton SA (2000) In vitro glucuronidation using human liver microsomes and the pore-forming peptide alamethicin. *Drug Metab Dispos* **28**:560–566.

García-Martín E, Martínez C, Tabarés B, Frias J, and Agúndez JA (2004) Interindividual variability in ibuprofen pharmacokinetics is related to interaction of cytochrome P450 2C8 and 2C9 amino acid polymorphisms. *Clin Pharmacol Ther* **76**:119–127.

Giacomini KM, Huang SM, Tweedie DJ, Benet LZ, Brouwer KL, Chu X, Dahlin A, Evers R, Fischer V, Hillgren KM, et al.; International Transporter Consortium (2010) Membrane transporters in drug development. *Nat Rev Drug Discov* **9**:215–236.

Hallifax D and Houston JB (2012) Evaluation of hepatic clearance prediction using in vitro data: emphasis on fraction unbound in plasma and drug ionisation using a database of 107 drugs. *J Pharm Sci* **101**:2645–2652.

Izumi S, Nozaki Y, Komori T, Takenaka O, Maeda K, Kusuhara H, and Sugiyama Y (2016) Investigation of fluorescein derivatives as substrates of organic anion transporting polypeptide (OATP) 1B1 to develop sensitive fluorescence-based OATP1B1 inhibition assays. *Mol Pharm* **13**:438–448.

Jones HM, Barton HA, Lai Y, Bi YA, Kimoto E, Kempshall S, Tate SC, El-Kattan A, Houston JB, Galetin A, et al. (2012) Mechanistic pharmacokinetic modeling for the prediction of transporter-mediated disposition in humans from sandwich culture human hepatocyte data. *Drug Metab Dispos* **40**:1007–1017.

Jones HM and Houston JB (2004) Substrate depletion approach for determining in vitro metabolic clearance: time dependencies in hepatocyte and microsomal incubations. *Drug Metab Dispos* **32**:973–982.

Kalvass JC and Maurer TS (2002) Influence of nonspecific brain and plasma binding on CNS exposure: implications for rational drug discovery. *Biopharm Drug Dispos* **23**:327–338.

Kato M, Chiba K, Hisaka A, Ishigami M, Kayama M, Mizuno N, Nagata Y, Takakuwa S, Tsukamoto Y, Ueda K, et al. (2003) The intestinal first-pass metabolism of substrates of CYP3A4 and P-glycoprotein-quantitative analysis based on information from the literature. *Drug Metab Pharmacokinet* **18**:365–372.

Kell DB, Dobson PD, and Oliver SG (2011) Pharmaceutical drug transport: the issues and the implications that it is essentially carrier-mediated only. *Drug Discov Today* **16**:704–714.

Kilford PJ, Stringer R, Sohal B, Houston JB, and Galetin A (2009) Prediction of drug clearance by glucuronidation from in vitro data: use of combined cytochrome P450 and UDP-glucuronosyltransferase cofactors in alamethicin-activated human liver microsomes. *Drug Metab Dispos* **37**:82–89.

Kimoto E, Bi YA, Kosa RE, Tremaine LM, and Varma MVS (2017) Hepatobiliary clearance prediction: species scaling from monkey, dog, and rat, and in vitro-in vivo

- extrapolation of sandwich-cultured human hepatocytes using 17 drugs. *J Pharm Sci* **106**:2795–2804.
- Kimoto E, Yoshida K, Balogh LM, Bi YA, Maeda K, El-Kattan A, Sugiyama Y, and Lai Y (2012) Characterization of organic anion transporting polypeptide (OATP) expression and its functional contribution to the uptake of substrates in human hepatocytes. *Mol Pharm* **9**:3535–3542.
- Kirchheiner J, Bauer S, Meineke I, Rohde W, Prang V, Meisel C, Roots I, and Brockmüller J (2002) Impact of CYP2C9 and CYP2C19 polymorphisms on tolbutamide kinetics and the insulin and glucose response in healthy volunteers. *Pharmacogenetics* **12**:101–109.
- Lepist EI, Zhang X, Hao J, Huang J, Kosaka A, Birkus G, Murray BP, Bannister R, Cihlar T, Huang Y, et al. (2014) Contribution of the organic anion transporter OAT2 to the renal active tubular secretion of creatinine and mechanism for serum creatinine elevations caused by cobicistat. *Kidney Int* **86**:350–357.
- Li R, Barton HA, and Varma MV (2014) Prediction of pharmacokinetics and drug-drug interactions when hepatic transporters are involved. *Clin Pharmacokinet* **53**: 659–678.
- Liu L and Pang KS (2005) The roles of transporters and enzymes in hepatic drug processing. *Drug Metab Dispos* **33**:1–9.
- Maeda K, Ikeda Y, Fujita T, Yoshida K, Azuma Y, Haruyama Y, Yamane N, Kumagai Y, and Sugiyama Y (2011) Identification of the rate-determining process in the hepatic clearance of atorvastatin in a clinical cassette microdosing study. *Clin Pharmacol Ther* **90**:575–581.
- Mathialagan S, Costales C, Tylaska L, Kimoto E, Vildhede A, Johnson J, Johnson N, Sarashina T, Hashizume K, Isringhausen CD, et al. (2018) In vitro studies with two human organic anion transporters: OAT2 and OAT7. *Xenobiotica* **48**:1037–1049.
- Mathialagan S, Piotrowski MA, Tess DA, Feng B, Litchfield J, and Varma MV (2017) Quantitative prediction of human renal clearance and drug-drug interactions of organic anion transporter substrates using in vitro transport data: a relative activity factor approach. *Drug Metab Dispos* **45**:409–417.
- Ménochet K, Kenworthy KE, Houston JB, and Galetin A (2012) Use of mechanistic modeling to assess interindividual variability and interspecies differences in active uptake in human and rat hepatocytes. *Drug Metab Dispos* **40**:1744–1756.
- Morgan RE, Trauner M, van Staden CJ, Lee PH, Ramachandran B, Eschenberg M, Afshari CA, Qualls CW Jr, Lightfoot-Dunn R, and Hamadeh HK (2010) Interference with bile salt export pump function is a susceptibility factor for human liver injury in drug development. *Toxicol Sci* **118**:485–500.
- Nakamura K, Hirayama-Kurogi M, Ito S, Kuno T, Yoneyama T, Obuchi W, Terasaki T, and Ohtsuki S (2016) Large-scale multiplex absolute protein quantification of drug-metabolizing enzymes and transporters in human intestine, liver, and kidney microsomes by SWATH-MS: comparison with MRM/SRM and HR-MRM/PRM. *Proteomics* **16**:2106–2117.
- Obach RS (1999) Prediction of human clearance of twenty-nine drugs from hepatic microsomal intrinsic clearance data: an examination of in vitro half-life approach and nonspecific binding to microsomes. *Drug Metab Dispos* **27**:1350–1359.
- Obach RS, Baxter JG, Liston TE, Silber BM, Jones BC, MacIntyre F, Rance DJ, and Wastall P (1997) The prediction of human pharmacokinetic parameters from preclinical and in vitro metabolism data. *J Pharmacol Exp Ther* **283**:46–58.
- Obach RS, Lombardo F, and Waters NJ (2008) Trend analysis of a database of intravenous pharmacokinetic parameters in humans for 670 drug compounds. *Drug Metab Dispos* **36**:1385–1405.
- Pang KS and Rowland M (1977) Hepatic clearance of drugs. II. Experimental evidence for acceptance of the “well-stirred” model over the “parallel tube” model using lidocaine in the perfused rat liver in situ preparation. *J Pharmacokinetic Biopharm* **5**:655–680.
- Patilea-Vrana G and Unadkat JD (2016) Transport vs. metabolism: what determines the pharmacokinetics and pharmacodynamics of drugs? Insights from the extended clearance model. *Clin Pharmacol Ther* **100**:413–418.
- Perini JA, Vianna-Jorge R, Brogliato AR, and Suarez-Kurtz G (2005) Influence of CYP2C9 genotypes on the pharmacokinetics and pharmacodynamics of piroxicam. *Clin Pharmacol Ther* **78**:362–369.
- Poirier A, Lavé T, Portmann R, Brun ME, Senner F, Kansy M, Grimm HP, and Funk C (2008) Design, data analysis, and simulation of in vitro drug transport kinetic experiments using a mechanistic in vitro model. *Drug Metab Dispos* **36**:2434–2444.
- Poulin P, Kenny JR, Hop CE, and Haddad S (2012) In vitro-in vivo extrapolation of clearance: modeling hepatic metabolic clearance of highly bound drugs and comparative assessment with existing calculation methods. *J Pharm Sci* **101**:838–851.
- Rettie AE, Wienkers LC, Gonzalez FJ, Trager WF, and Korzekwa KR (1994) Impaired (S)-warfarin metabolism catalysed by the R144C allelic variant of CYP2C9. *Pharmacogenetics* **4**:39–42.
- Roth M, Timmermann BN, and Hagenbuch B (2011) Interactions of green tea catechins with organic anion-transporting polypeptides. *Drug Metab Dispos* **39**: 920–926.
- Scordo MG, Pengo V, Spina E, Dahl ML, Gusella M, and Padriani R (2002) Influence of CYP2C9 and CYP2C19 genetic polymorphisms on warfarin maintenance dose and metabolic clearance. *Clin Pharmacol Ther* **72**:702–710.
- Shen H, Lai Y, and Rodrigues AD (2017) Organic anion transporter 2 (OAT2): an enigmatic human solute carrier. *Drug Metab Dispos* **45**:228–236.
- Shitara Y, Horie T, and Sugiyama Y (2006) Transporters as a determinant of drug clearance and tissue distribution. *Eur J Pharm Sci* **27**:425–446.
- Shitara Y, Maeda K, Ikejiri K, Yoshida K, Horie T, and Sugiyama Y (2013) Clinical significance of organic anion transporting polypeptides (OATPs) in drug disposition: their roles in hepatic clearance and intestinal absorption. *Biopharm Drug Dispos* **34**:45–78.
- Shitara Y and Sugiyama Y (2006) Pharmacokinetic and pharmacodynamic alterations of 3-hydroxy-3-methylglutaryl coenzyme A (HMG-CoA) reductase inhibitors: drug-drug interactions and interindividual differences in transporter and metabolic enzyme functions. *Pharmacol Ther* **112**:71–105.
- Simons K and Ikonen E (1997) Functional rafts in cell membranes. *Nature* **387**: 569–572.
- Srianni GL and Pang KS (1997) Organ clearance concepts: new perspectives on old principles. *J Pharmacokinetic Biopharm* **25**:449–470.
- Sohlenius-Sternbeck AK (2006) Determination of the hepatocellularity number for human, dog, rabbit, rat and mouse livers from protein concentration measurements. *Toxicol In Vitro* **20**:1582–1586.
- Takanohashi T, Kubo S, Arisaka H, Shinkai K, and Ubukata K (2012) Contribution of organic anion transporting polypeptide (OATP) 1B1 and OATP1B3 to hepatic uptake of nateglinide, and the prediction of drug-drug interactions via these transporters. *J Pharm Pharmacol* **64**:199–206.
- Varma MV, Bi YA, Kimoto E, and Lin J (2014) Quantitative prediction of transporter- and enzyme-mediated clinical drug-drug interactions of organic anion-transporting polypeptide 1B1 substrates using a mechanistic net-effect model. *J Pharmacol Exp Ther* **351**:214–223.
- Varma MV, Chang G, Lai Y, Feng B, El-Kattan AF, Litchfield J, and Goosen TC (2012a) Physicochemical property space of hepatobiliary transport and computational models for predicting rat biliary excretion. *Drug Metab Dispos* **40**: 1527–1537.
- Varma MV, El-Kattan AF, Feng B, Steyn SJ, Maurer TS, Scott DO, Rodrigues AD, and Tremaine LM (2017a) Extended Clearance Classification System (ECCS) informed approach for evaluating investigational drugs as substrates of drug transporters. *Clin Pharmacol Ther* **102**:33–36.
- Varma MV, Feng B, Obach RS, Troutman MD, Chupka J, Miller HR, and El-Kattan A (2009) Physicochemical determinants of human renal clearance. *J Med Chem* **52**: 4844–4852.
- Varma MV, Lai Y, and El-Kattan AF (2017b) Molecular properties associated with transporter-mediated drug disposition. *Adv Drug Deliv Rev* **116**:92–99.
- Varma MV, Lai Y, Feng B, Litchfield J, Goosen TC, and Bergman A (2012b) Physiologically based modeling of pravastatin transporter-mediated hepatobiliary disposition and drug-drug interactions. *Pharm Res* **29**:2860–2873.
- Varma MV, Lin J, Bi YA, Rotter CJ, Fahmi OA, Lam JL, El-Kattan AF, Goosen TC, and Lai Y (2013) Quantitative prediction of repaglinide-rifampin complex drug interactions using dynamic and static mechanistic models: delineating differential CYP3A4 induction and OATP1B1 inhibition potential of rifampin. *Drug Metab Dispos* **41**:966–974.
- Varma MV, Steyn SJ, Allerton C, and El-Kattan AF (2015) Predicting clearance mechanism in drug discovery: extended clearance classification system (ECCS). *Pharm Res* **32**:3785–3802.
- Vildhede A, Kimoto E, Rodrigues AD, and Varma MVS (2018) Quantification of hepatic organic anion transport proteins OAT2 and OAT7 in human liver tissue and primary hepatocytes. *Mol Pharm* **15**:3227–3235.
- Walsky RL, Bauman JN, Bourcier K, Giddens G, Lapham K, Negahban A, Ryder TF, Obach RS, Hyland R, and Goosen TC (2012) Optimized assays for human UDP-glucuronosyltransferase (UGT) activities: altered alamethicin concentration and utility to screen for UGT inhibitors. *Drug Metab Dispos* **40**:1051–1065.
- Watanabe T, Kusuhara H, Maeda K, Kanamaru H, Saito Y, Hu Z, and Sugiyama Y (2010) Investigation of the rate-determining process in the hepatic elimination of HMG-CoA reductase inhibitors in rats and humans. *Drug Metab Dispos* **38**: 215–222.
- Wood FL, Houston JB, and Hallifax D (2017) Clearance prediction methodology needs fundamental improvement: trends common to rat and human hepatocytes/microsomes and implications for experimental methodology. *Drug Metab Dispos* **45**:1178–1188.
- Yoshikado T, Maeda K, Furihata S, Terashima H, Nakayama T, Ishigame K, Tsunemoto K, Kusuhara H, Furihata KI, and Sugiyama Y (2017) A clinical cassette dosing study for evaluating the contribution of hepatic OATPs and CYP3A to drug-drug interactions. *Pharm Res* **34**:1570–1583.
- Zhang Y, Han Y-H, Putluru SP, Matta MK, Kole P, Mandekar S, Furlong MT, Liu T, Iyer RA, Marathe P, et al. (2016) Diclofenac and its acyl glucuronide: determination of in vivo exposure in human subjects and characterization as human drug transporter substrates in vitro. *Drug Metab Dispos* **44**:320–328.
- Zheng HX, Huang Y, Frassetto LA, and Benet LZ (2009) Elucidating rifampin's inducing and inhibiting effects on glyburide pharmacokinetics and blood glucose in healthy volunteers: unmasking the differential effects of enzyme induction and transporter inhibition for a drug and its primary metabolite. *Clin Pharmacol Ther* **85**:78–85.

Address correspondence to: Manthana V. S. Varma, ADME Sciences, Medicine Design, Worldwide Research and Development, MS 8220-2451, Pfizer Inc., Groton, CT 06340. E-mail: manthana.v.varma@pfizer.com

**Organic Anion Transporter 2 mediated Hepatic Uptake Contribute to the Clearance of High Permeability–
Low Molecular Weight Acid and Zwitterion Drugs: Evaluation using 25 drugs.**

Emi Kimoto, Sumathy Mathialagan, Laurie Tylaska, Mark Niosi, Jian Lin, Anthony Carlo, David Tess, Manthena V. S. Varma

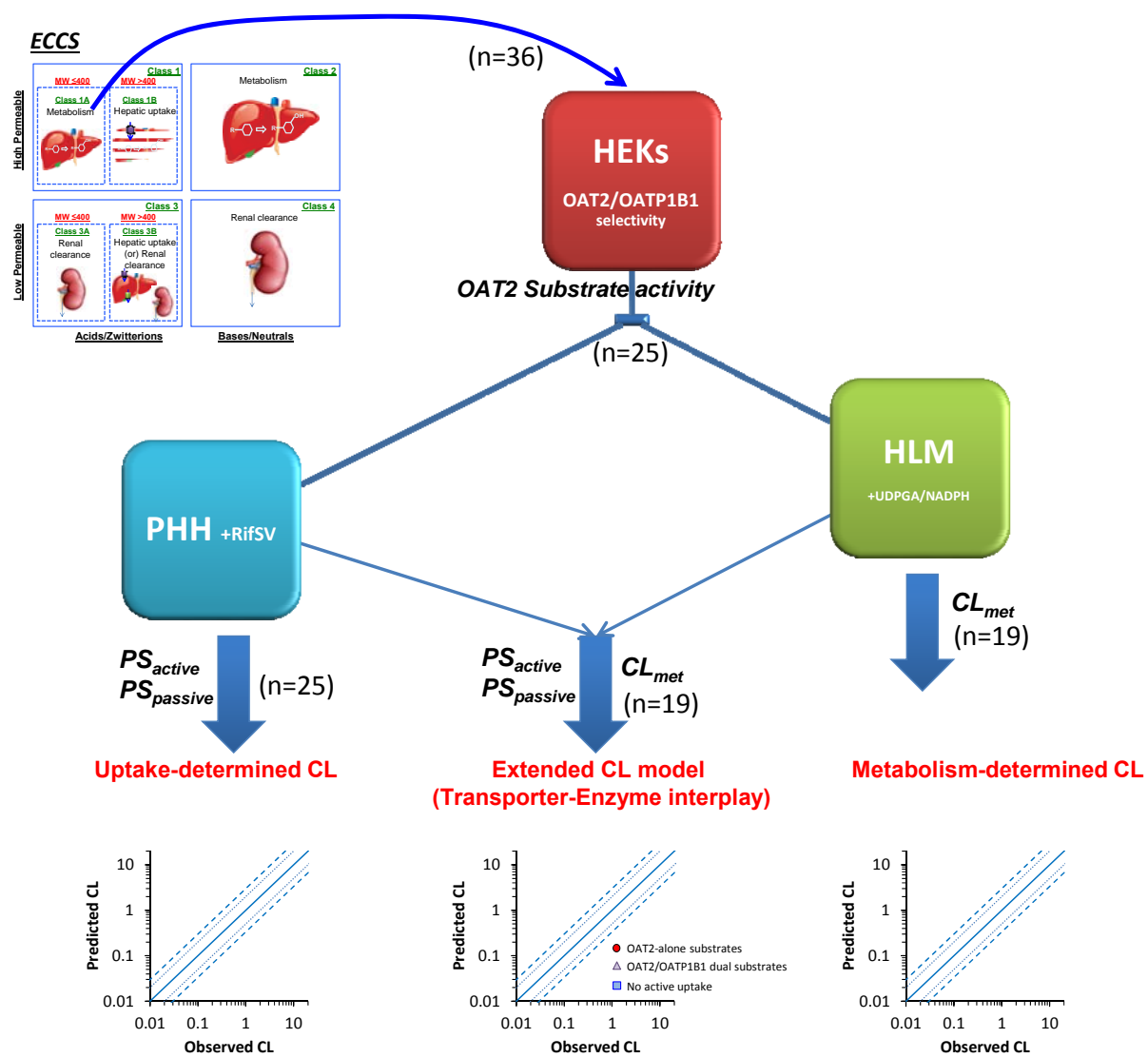
ADME Sciences, Medicine Design, Worldwide Research and Development, Pfizer Inc., Groton, CT 06340.

Supplemental Table 1. LC-MS/MS conditions for sample analysis in metabolism studies.

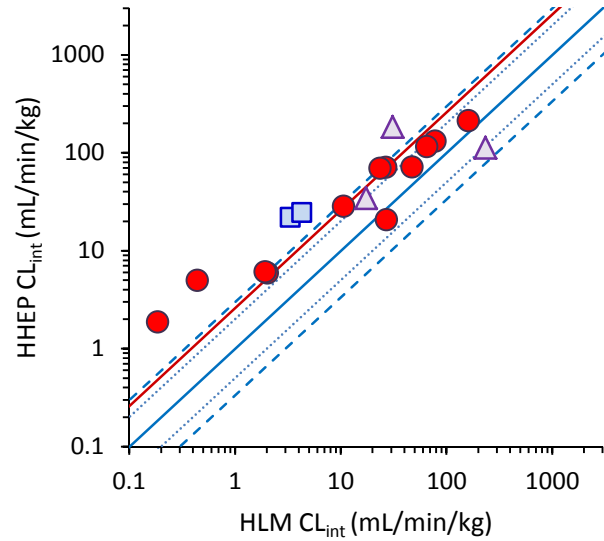
Compound	Analyte		Detection Mode	Declustering Potential	Collision Energy	Gradient Program	Flow Rate	Column
	m/z transition							
	Q1	Q3		(eV)	(eV)	%B (min)	mL/min	
Aminosalicilic acid	152	108	Negative	-50	-20	2(0) → 98(2.5) → 2(0.5)	0.5	Ace
Bromfenac	335	289	Positive	83	10	10(0) → 100(1.75) → 10(1.7)	0.4	Kinetex
Carbamazepine (IS for positive mode)	237	194	Positive	140	30	10(0) → 100(1.75) → 10(1.7)	0.4	Kinetex
Clinafloxin	366	305	Positive	60	27	5(0) → 95(2.5) → 5(0.5)	0.5	Ace
CP-628374 (IS for positive mode)	687	320	Positive	190	35	10(0) → 100(1.75) → 10(1.7)	0.4	Kinetex
CP-628374 (IS for negative mode)	685	149	Negative	-200	-58	10(0) → 100(1.75) → 10(1.7)	0.4	Kinetex
Diclofenac	296	215	Positive	60	26	5(0) → 95(2.5) → 5(0.5)	0.5	Ace
Enalaprilat	349	117	Positive	70	45	2(0) → 98(2.5) → 2(0.5)	0.5	Ace
Entacapone	304	184	Negative	-75	-45	2(0) → 98(2.5) → 2(0.5)	0.5	Ace
Fenoprofen	241	197	Negative	-35	-15	2(0) → 98(2.5) → 2(0.5)	0.5	Halo
Fluorescein	333	202	Positive	100	60	10(0) → 100(1.75) → 10(1.7)	0.4	Kinetex
Gemfibrozil	249	121	Negative	-50	-20	10(0) → 100(1.75) → 10(1.7)	0.4	Kinetex
Gliclazide	324	127	Positive	90	30	10(0) → 100(1.75) → 10(1.7)	0.4	Kinetex
Ibuprofen	205	161	Negative	-30	-10	10(0) → 100(1.75) → 10(1.7)	0.4	Kinetex
Indomethacin	356	312	Negative	-50	-15	2(0) → 98(2.5) → 2(0.5)	0.5	Ace
Milrinone	212	140	Positive	130	47	2(0) → 98(2.5) → 2(0.5)	0.5	Ace
Naproxen	231	147	Positive	50	25	10(0) → 100(1.75) → 10(1.7)	0.4	Kinetex
Nateglinide	318	166	Positive	100	17	10(0) → 100(1.75) → 10(1.7)	0.4	Kinetex
Pioglitazone	357	134	Positive	50	12	2(0) → 98(2.5) → 2(0.5)	0.5	Ace
Pralidoxime	137	119	Positive	60	30	10(0) → 100(1.75) → 10(1.7)	0.4	Kinetex
Rosiglitazone	358	135	Positive	60	21	2(0) → 98(2.5) → 2(0.5)	0.5	Ace
Sulfamethoxazole	254	156	Positive	100	17	2(0) → 98(2.5) → 2(0.5)	0.5	Ace
Terfenadine	472	436	Positive	80	35	5(0) → 95(2.5) → 5(0.5)	0.5	Ace
Thalidomide	259	84	Positive	70	20	2(0) → 98(2.5) → 2(0.5)	0.6	Ace
Tiagabine	376	111	Positive	140	55	10(0) → 100(1.75) → 10(1.7)	0.4	Kinetex
Tolbutamide (IS for negative mode)	269	170	Negative	-50	-28	2(0) → 98(2.5) → 2(0.5)	0.5	Halo
Tolcapone	272	181	Negative	-70	-30	10(0) → 99(2.5) → 10(0.5)	0.5	Halo

Warfarin	309	251	Positive	98	25	10(0) → 100(1.75) → 10(1.7)	0.4	Kinetex
Isoxicam	336.2	99	Positive	100	20	10(0) → 100(1.75) → 10(1.7)	0.5	Kinetex
Piroxicam	332.2	95	positive	70	25	10(0) → 100(1.75) → 10(1.7)	0.5	Kinetex

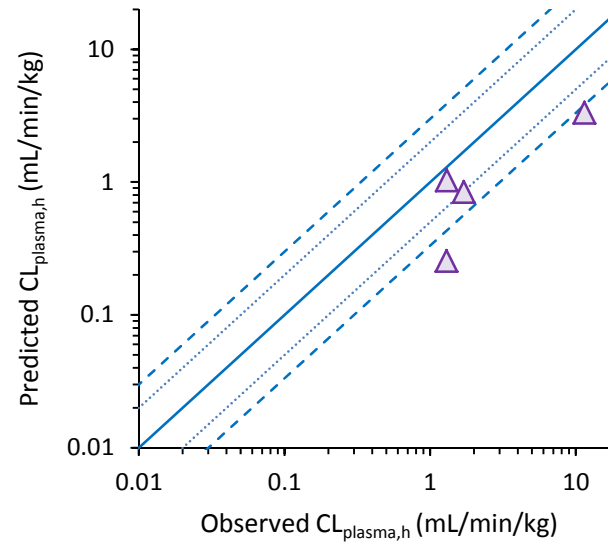
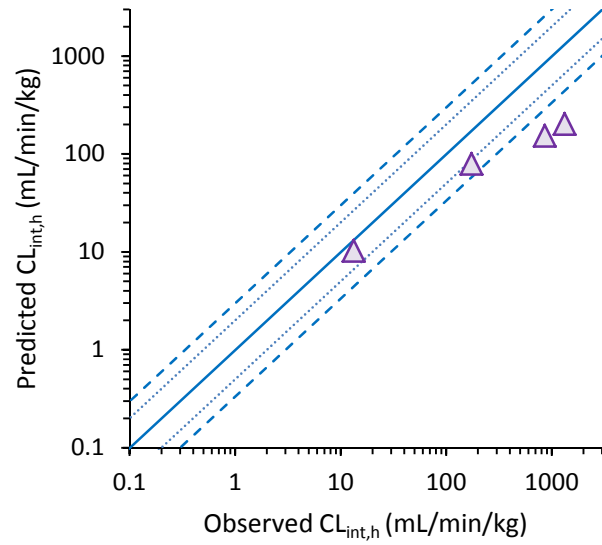
In terms of LC-MS/MS condition for uptake clearance study in PHH and transfected HEK cells, samples (10 μ L) were injected onto a Kinetex C18 column (2.6 μ m, 100 Å, 30 \times 2.1 mm, Phenomenex, Torrance, CA) and eluted by mobile phase with initial conditions of 10% solvent B for 0.2 minute, followed by a linear gradient of 10% solvent B to 100% solvent B over 1.05 minute, followed by the washing step using 100% mobile solvent B for 0.5 minute, and re-equilibration for 0.75 minute (solvent A: 100% water with 0.1% formic acid; solvent B: 100% ACN with 0.1% formic acid) at a flow rate of 0.4 mL/min. The mass transitions for monitoring substrates were in Supplemental Table 1.



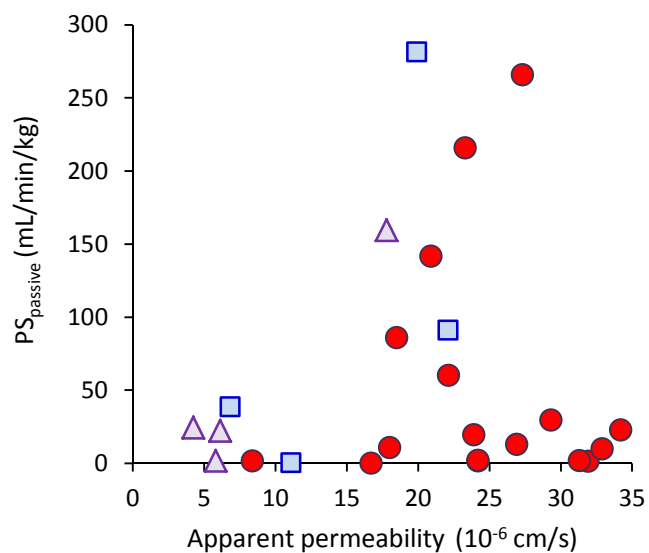
Supplemental Figure 1. Schematic of the step-wise approach employed in evaluating the clearance mechanism of high permeability-low molecular weight acid and zwitterion drugs (ECCS class 1A).



Supplemental Figure 2. Comparison of intrinsic clearance measured by substrate-depletion in pooled human liver microsomes and pooled human hepatocytes. Values are corrected for the $f_{u,mic}$ or $f_{u,inc}$. Circles represent OAT2-alone substrates, triangles represent OAT2/OATP1B1 dual substrates, and squares represent drugs with no measurable active uptake in human hepatocytes. Solid, dotted and dashed diagonal blue lines indicate unity, 2-fold, and 3-fold range, respectively. Red diagonal line represent bias for OAT2-alone substrates.



Supplemental Figure 3. Observed versus predicted clearance of the 4 OAT2/OATP1B1 dual substrates assuming an empirical scaling factor of 10.6 (Varma et al., 2014) for the active hepatic uptake (PS_{active}) in the extended clearance model (Eq. 10). Left and right panels represent hepatic intrinsic clearance and hepatic plasma clearance, respectively. Solid, dotted and dashed diagonal blue lines indicate unity, 2-fold, and 3-fold range, respectively. Red diagonal line represents bias.



Supplemental Figure 4. Comparison of apparent transcellular permeability (P_{app}) across MDCK-low efflux cell monolayers with the passive hepatic uptake clearance ($PS_{passive}$) measured using plated human hepatocytes. Circles represent OAT2-alone substrates, triangles represent OAT2/OATP1B1 dual substrates, and squares represent drugs with no measurable active uptake in human hepatocytes.